Accepted Manuscript

Design, synthesis, biological evaluation and molecular docking studies of phenylpropanoid derivatives as potent anti-hepatitis B virus agents

Sheng Liu, Wanxing Wei, Yubin Li, Xu Liu, Xiaoji Cao, Kechan Lei, Min Zhou

PII: S0223-5234(15)00223-8

DOI: 10.1016/j.ejmech.2015.03.056

Reference: EJMECH 7801

To appear in: *European Journal of Medicinal Chemistry*

Received Date: 5 November 2014

Revised Date: 24 March 2015

Accepted Date: 25 March 2015

Please cite this article as: S. Liu, W. Wei, Y. Li, X. Liu, X. Cao, K. Lei, M. Zhou, Design, synthesis, biological evaluation and molecular docking studies of phenylpropanoid derivatives as potent anti-hepatitis B virus agents, *European Journal of Medicinal Chemistry* (2015), doi: 10.1016/j.ejmech.2015.03.056.

A series of phenylpropanoid derivatives were discovered as potent anti-HBV agents. Compound 4c-1 showed the most potent anti-HBV activity, demonstrating potent inhibitory effect not only on the secretion of HBsAg (IC_{50} = 14.18 μM, SI = 17.85) and HBeAg (IC_{50} = 6.20 μM, SI = 40.82) secretion but also HBV DNA replication (IC_{50} = 23.43 μM, SI = 10.80). The structure-activity relationships of were analysed and docking study was carried out to explore the molecular interactions and a molecular target by MOE.

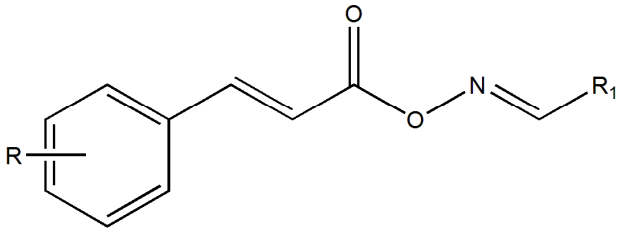

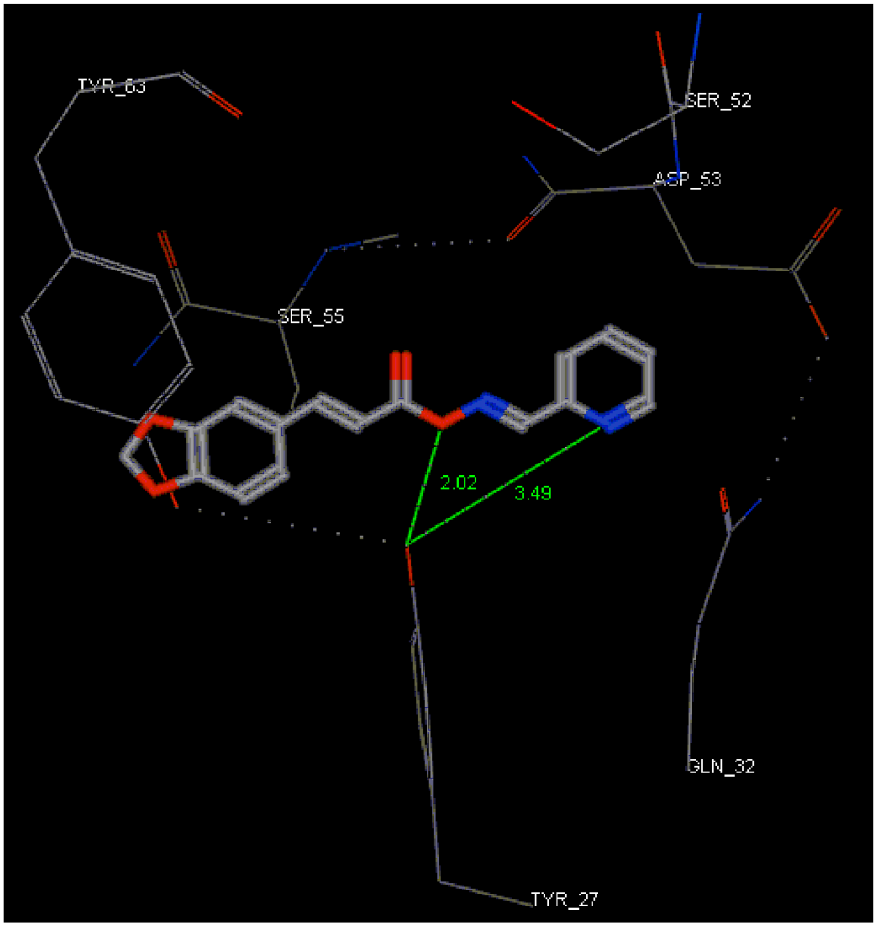

Design, synthesis, biological evaluation and molecular docking studies of phenylpropanoid derivatives as potent anti-hepatitis B virus agents

Sheng Liu[1], Wanxing Wei *[1], Yubin Li[2], Xu Liu[1], Xiaoji Cao[3], Kechan Lei[1], Min Zhou[1]

[1]Department of Chemistry, Guangxi University, Nanning, 530004, P. R. China

[2]School of Chemistry and Chemical Engineering, Sun Yat-Sen University, Guangzhou 510275, P. R. China

[3]Center of Analysis and Testing, Zhejiang University of Industry, Hangzhou, 310014, P. R. China

*Corresponding author. Tel.: +86 7713272601. fax +86 7713272601. E-mail: wxwei@gxu.edu.cn (W. Wei)

Abstract: A series of phenylpropanoid derivatives were synthesized, and their anti-hepatitis B virus (HBV) activity was evaluated in HepG 2.2.15 cells. Most of the synthesized derivatives showed effective anti-HBV activity. Of these compounds, compound 4c-1 showed the most potent anti-HBV activity, demonstrating potent inhibitory effect not only on the secretion of HBsAg (IC_{50} = 14.18 μM, SI = 17.85) and HBeAg (IC_{50} = 6.20 μM, SI = 40.82) secretion but also HBV DNA replication (IC_{50} = 23.43 μM, SI = 10.80). The structure-activity relationships (SARs) of phenylpropanoid derivatives had been discussed, which were useful for phenylpropanoid derivatives to be explored and developed as novel anti-HBV agents. Moreover, the docking study of all synthesized compounds inside the HLA-A protein (PDB ID: 3OX8) active site were carried out to explore the molecular interactions and a molecular target for activity of phenylpropanoid derivatives with the protein using a moe-docking technique. This study identified a new class of potent anti-HBV agents.

Keywords: Synthesis, Phenylpropanoid derivatives, Anti-HBV activity, Structure-activity relationships, Molecular docking

1. Introduction

Hepatitis B virus (HBV) infection is a serious worldwide health problem, which can cause both acute and chronic infections of the liver and may lead to lifelong infection, cirrhosis, hepatocellular carcinoma, liver failure, or death [1, 2]. There are about 350-400 million people worldwide are chronically infected with HBV with 0.5-1.2 million global deaths per year [3]. Currently, therapies including immunomodulator, interferons (interferon-alpha and pegylated interferon), and nucleoside drugs (lamivudine, adefovir dipivoxil, entecavir, telbivudine and tenofovir) for treating HBV are still unsatisfactory, due to high recurrence, drug resistance and inevitable side effects [4]. Therefore, there exists a significant unmet medical need to explore novel classes of drugs with different antiviral targets and mechanisms for anti-HBV purposes.

Natural products and their derivatives possessing various skeletons could provide a great opportunity for finding novel HBV inhibitors [5-9]. In our continuing research for *Phyllanthus niruri L.*, a traditional Chinese medicinal herb used in folk medicine for liver protection and antihepatitis B, anti-HBV active constituents, such as niranthin, nirtetralin, nirtetralin A and nirtetralin B, were investigated [10-12]. In view of their novel structural template, which differs from those of all reported anti-HBV agents, we designed and synthesized a series of analogues in order to screen and determine structure-activity relationships (SARs) and develop more potent anti-HBV agents. As the facts that the anti-HBV active lignans possess the same structural fragment, 3,4-dimethoxyphenyl, 3,4,5-trimethoxyphenyl, benzo[d][1,3]dioxol-5-yl, or 4-methoxybenzo[d][1,3]dioxole-5-yl, in their molecular structures, we selected (E)-3-(3,4-dimethoxyphenyl)acrylic acid (a),

(E)-3-(3,4,5-trimethoxyphenyl)acrylic acid (b), (E)-3-(benzo[d][1,3]dioxol-5-yl)acrylic acid (c) and (E)-3-(7-methoxybenzo[d][1,3]dioxol-5-yl)acrylic acid (d) as the main scaffold for the design and synthesis of novel compounds as potent anti-HBV agents. According to molecular hybridization principle, esterification of natural compounds is an effective approach for achieving promising derivatives, by which two active parts can be easily hybridized to enhance activity [13, 14]. Some derivatives of the four acrylic acids were synthesized for treatment of HIV, antiproliferative activity, antioxidation and antitumor activity [15-18], and some non-nucleoside anti-HBV agents such as isoflavone analogs also have been reported [19-21], but no investigation was concerned with phenylpropanoid analogs for HBV activity. Consequently, our efforts were devoted to design, synthesize, pharmacological evaluation in vitro and SARs elucidation of a series of phenyl acryloyl type oxime esters based on the four acrylic acids as anti-HBV agents.

A QSAR study was carried out for all the series of molecules to help in early preclinical development and avoid costly late-stage preclinical [22, 23]. In addition, attempt to elucidate the molecular interactions and a molecular target for activity was achieved by molecular docking of all synthesized compounds into the active site using molecular operating environment (MOE).

2. Results and Discussion

2.1. Chemistry

General synthesis for the intermediate and target compounds is depicted in Scheme 1. Substituted benzaldehyde was reacted with hydroxylamine hydrochloride in EtOH

in the presence of sodium acetate to yield oxime 1-3 in a good yield [24]. Intermediates 2a-d were prepared by Knoevenagel condensation of malonic acid and the aldehyde group of four benzaldehydes with yields of 80%-90% [25]. The final oxime ester derivatives (4a-1~ 4a-3), (4b-1~ 4b-3), (4c-1~ 4c-3), (4d-1~ 4d-3) were obtained by reaction of oxime with cinnamoyl chloride 3a-d in the presence of TEA, which was obtained by reaction of substituted phenylacrylic acid 2a-d and thionyl chloride in DCM [26].

The structures of the newly synthesized compounds (4a-1~ 4a-3), (4b-1~ 4b-3), (4c-1~ 4c-3), (4d-1~ 4d-3) were characterized by ^{1}H NMR, ^{13}CNMR and MS data and their data are presented in the experimental section. ^{1}H NMR spectra of the derivatives showed a singlet at about 8.35-8.76 ppm corresponding to N=CH proton. Two doublets at 6.37-6.74 and 7.53-7.84 ppm with J=15.25-15.91 Hz corresponding to trans hydrogens of CH=CH respectively. The singlet at 3.89-3.96 ppm attributed to O-CH_3 protons, and at 6.00-6.04 corresponded to OCH_2O protons. The chemical shifts of aromatic hydrogens of the phenyl ring appeared as multiplets in the region δ 6.67-7.21. ^{13}C NMR chemical shifts for title compounds were observed in their expected regions. ^{13}C NMR spectrum for the derivatives showed signals at 55.26-61.00, 101.45-102.12, 155.15-160.04 and 162.31-165.92 corresponding to CH_3, CH_2, C=N and C=O, respectively.

2.2. QSAR study

The 3D structures of all the compounds were generated using the Built Optimum option of Hyperchem software (version 8.0), and subsequently energy minimized using MM+ force field. Then, the structures were fully optimized. Molecular descriptors were determined by

QSAR study, including logP, molar refractivity, surface area, volume, hydration energy and polarizability, and the results showing that all molecules have drug like properties (Table 1). All the compounds have the molecular weight ranging from 285 to 350 Da. The log P values of these compounds are superior to act as drug which is -2.14 to 0.80 and the molar refractivity is in the range of 80-100.

2.3. Molecular docking

Molecular docking studies of phenylpropanoid derivatives were carried out using MOE 2008.10 as docking software in order to rationalize biological activity results and understand the various interactions between ligand and protein in the active site in detail. The crystal structure of HLA-A protein (PDB ID: 3OX8), which was associated with severe liver inflammation in Chinese patients with chronic HBV infection, was used for docking study. And the 'Site Finder' tool of the program was used to search for its active site. We performed three docking procedures for each ligand and the best configuration of each of the ligand-receptor complexes was selected based on energetic grounds. The affinity scoring function δG was used to assess and rank the receptor-ligand complexes. The docking scores and the hydrogen bonding strength of all the molecules were shown in Table 2.

The synthesized series derivatives had dock score ranging from -12.4670 to -18.3979. Compound 4c-1 was showing the best least docking score of -18.3979 and the next best least docking score was found with 4d-1 followed by 4d-2. Two hydrogen bonds were present in the derivative 4a-1, 4b-1 and 4c-1, which was the highest among the series. Compound 4c-1 was found to be forming two hydrogen bonds of lengths 2.02 and 3.49 Å each with O of O-N

in the oxime ester group and N in pyridine ring of Tyr27 respectively (Fig. 1). Compound 4d-1 only formed one hydrogen bond of length 3.03 Å with O-N in oxime ester group of Tyr27 (Fig. 2). Compound 4d-2 also formed only one hydrogen bond of bond length 2.87 Å with O-N in oxime ester group of Tyr27 (Fig. 3). The compounds 4c-1, 4d-1 and 4d-2 exhibited the best least docking score had good in vitro anti-HBV activity.

2.4. Anti-HBV activity

All the newly synthesized derivatives were tested for their anti-HBV activity, namely inhibiting the secretion of HBsAg, and HBeAg in HepG 2.2.15 cells using lamivudine (3TC, a clinically popular anti-HBV agent) as a positive control. The anti-HBV activity of each compound was expressed as the concentration of compound that achieved 50% inhibition (IC_{50}) to the secretion of HBsAg and HBeAg. And the cytotoxicity of each compound was expressed as the concentration of compound required to kill 50% (CC_{50}) of the HepG 2.2.15 cells. The selectivity index (SI), a major pharmaceutical parameter that estimates possible future clinical development, was determined as the ratio of CC_{50} to IC_{50}. The results of their anti-HBV activity and cytotoxicity were listed in Table 3.

The treatment of HBV-transfected HepG2.2.15 cells with various concentrations of drugs for 9 d exhibited a time-and dose-dependent inhibitory effect on the secretion of HBsAg and HBeAg (Fig. 4). In synthesized derivatives, all compounds showed better activity inhibiting the secretion of HBsAg than that of lamivudine. And eleven of twelve derivatives, with higher inhibitory activity against the secretion of HBeAg than lamivudine were obtained except for 4a-3. Compound 4c-1 showed the most potent anti-HBV activity, demonstrating potent

inhibitory effect on the secretion of HBsAg (IC_{50} = 14.08 μM, SI = 17.85) and HBeAg (IC_{50} = 6.20 μM, SI = 40.82) but appeared toxic (CC_{50} = 253.11 μM). Compound 4d-1 showed the next most potent inhibitory to the secretion of HBsAg (IC_{50}=62.79 μM) and HBeAg (IC_{50} = 72.91 μM). Compared to compound 4d-1, compound 4d-2 relatively low inhibitory potency to the secretion of HBsAg (IC_{50} = 63.51 μM) and HBeAg (IC_{50} = 75.26 μM), but weak toxic (CC_{50} = 819.58 μM) led to relatively high SI values (SI_{HBsAg} = 12.90, SI_{HBeAg} = 10.89).

Importantly, the most active compounds 4c-1, 4c-2, 4d-1, 4d-2 and 4d-3 with high activities against HBsAg and HBeAg were selected to investigate inhibition of HBV DNA replication using lamivudine as the reference drug. Compounds 4c-1, 4d-1, and 4d-2 exhibited anti-HBV activity with their IC_{50} values against HBV DNA replication of 23.43, 95.04, 139.73 μM, respectively. Compounds 4c-1, 4d-1, and 4d-2 displayed inhibiting not only HBsAg and HBeAg secretion but also HBV DNA replication, however, 3TC showed significantly activity against HBV DNA replication (IC_{50} = 6.86) while showed little inhibitory on HBsAg and HBeAg secretion.

2.5. Structure-activity relationship

The start reactants substituted benzaldehyde 1a-d, intermediates 2a-d and oximes 1-3 showed low suppressant properties on the HBV while most of the derivatives showed high potency activity against of the secretion of HBsAg and HBeAg as shown in Table 3. In the docking study, we also found that the O of O-N in the oxime ester group interacted with Tyr27 by hydrogen bond. It indicated that oxime ester group (O=C-O-N=C) of the newly synthesized derivatives might be a good target for further

lead optimization by introduction the rational substitutions.

Derivatives 4a-1 to 4d-1, 4a-2 to 4d-2 and 4a-3 to 4d-3 with the same oxime groups respectively showed different anti-HBV activity and cytotoxicity. Derivative 4d-2, with IC_{50} values of 63.51 μM and 75.26 μM for HBsAg and HBeAg respectively, was showing the most effective on inhibiting HBsAg and HBeAg secretion and the next was 4c-2 (HBsAg IC_{50} = 64.60 μM, HBeAg IC_{50} = 81.83 μM), followed by 4b-2 (HBsAg IC_{50} = 173.31 μM, HBeAg IC_{50} = 189.67 μM). It was similar to the derivatives 4a-1 to 4d-1 and 4a-3 to 4d-3 except that compound 4c-1 (HBsAg IC_{50}=14.18 μM, HBeAg IC_{50} = 6.20 μM) was observed to show more effective on inhibiting HBsAg and HBeAg secretion than that of 4d-1 (HBsAg IC_{50} = 62.79 μM, HBeAg IC_{50} = 72.91 μM) for its high cytotoxicity. Thus, after methoxy group introduced to the 5-C of cinnamoyl group, the inhibitory effect of compounds 4b-1, 4b-2 and 4b-3 on secretion of HBsAg and HBeAg slightly increased comparing to compounds 4a-1, 4a-2 and 4a-3 respectively. The introduction of the methoxy group to 5-C of 4d-1, 4d-2, and 4d-3 could also increase their anti-HBV activity comparing to compounds 4c-1, 4c-2 and 4c-3 respectively. The substituent of 3,4-dimethoxy by 3,4-methylenedioxy could increase their inhibitory effect on secretion of HBsAg and HBeAg compared 4a-1~3 with 4c-1~3, and 4b-1~3 with 4d-1~3. Compound 4a-2 displayed more cytotoxicity (CC_{50} = 624.24 μM) than 4b-2 (CC_{50} = 1049.90 μM) and 4c-2 possessed higher cytotoxicity (CC_{50} = 479.62 μM) than 4d-2 (CC_{50} = 819.58 μM), which indicated that the introduction of the methoxy group to 5-C could decrease cytotoxicity. Then, the cytotoxicity of 4c-2 was still stronger than that of 4a-2 and that of 4d-2 also stronger than 4b-2, indicating that the substituent of 3,4-dimethoxy by 3,4-methylenedioxy could increase the cytotoxicity. From the above results, it is indicated

193 that the introduction of methoxy group to 5-C could enhance the anti-HBV activity and
194 decrease cytotoxicity along with the high SI values, and the substituent of 3,4-dimethoxy by
195 3,4-methylenedioxy could increase activity and cytotoxicity along with relatively low SI
196 values.

197 Derivatives 4a-1~3, 4b-1~3, 4c-1~3 and 4d-1~3 contained the same phenylpropanoid part
198 respectively. 4a-1 showed the best anti-HBV activity (HBsAg IC_{50} = 151.87 μM, HBeAg IC_{50}
199 = 161.74 μM) and the next was 4a-2 (HBsAg IC_{50} = 191.26 μM, HBeAg IC_{50} = 201.65 μM),
200 followed by 4a-3 (HBsAg IC_{50} = 228.67 μM, HBeAg IC_{50} = 377.87 μM). The order also
201 applied to 4b-1~3, 4c-1~3 and 4d-1~3. It suggested that the introduction of pyridine showed
202 relatively high potent anti-HBV activity than introduction of furan and thiophene. Compound
203 4a-1 showed cytotoxicity with CC_{50} values of 545.16 μM. The cytotoxicity of derivatives 4a-3
204 (CC_{50} = 574.33 μM) decreased with thiophene group. Compound 4a-2 (CC_{50} = 624.24 μM)
205 was observed with the weakest cytotoxicity with furan group. Actually, all the derivatives
206 obtained from oxime 2 did show weakest cytotoxicity, followed by that from oxime 3. It
207 indicated that the introduction of pyridine group could enhance the anti-HBV activity but
208 increase the cytotoxicity.

209 According to the results mentioned above, SARs were summarized as followed: (1)
210 5-OCH_3-substituted compounds with methylenedioxy at 13,14-C could provide higher
211 anti-HBV activity than other analogues. (1) The anti-HBV activity of oxime-substituted
212 compounds could be pyridine-substituted > furan-substituted > thiophene-substituted.

213 **3. Conclusion**

In summary, our design and synthesis have led to a series of non-nucleoside anti-HBV agents by attaching of the oximes to cinnamic acids. Most of the derivatives displayed potent anti-HBV activity with the SI_{HBsAg} values from 2.51 to 12.90 and SI_{HBeAg} values from 1.52 to 27.92. Interestingly, compounds 4c-1, 4d-1, and 4d-2 displayed inhibiting not only HBsAg and HBeAg secretion but also HBV DNA replication, however, 3TC showed significantly activity against HBV DNA replication. In addition, the docking study of the tested compounds inside the HLA-A protein active site was predicted using a moe-docking technique. The results of the in vitro anti-HBV activity study were consistent with the docking results indicating that the anti-HBV effect of the prepared compounds may exert its anti-HBV activity by inhibiting HLA-A. This study identified a new class of potent anti-HBV agents and offered valuable information for seeking non-nucleoside anti-HBV drug candidates.

4. Materials and methods

4.1. General

Melting points were determined using electrothermal melting point apparatus WRX-4 (Shanghai, China) and were uncorrected. MS spectra were run on a Finnigan LCQ Deca XP MAX mass spectrometer (Thermo Fisher, San Jose, CA, USA) equipped with an ESI source and an ion trap analyzer in the positive ion mode/in the negative ion. NMR spectra were recorded on Bruker AM 400 MHz ($^1H/^{13}C$, 400 MHz/100 MHz) or Bruker DRX 500 MHz ($^1H/^{13}C$, 500 MHz/125 MHz) spectrometer (Bruker, Bremerhaven, Germany) and chemical shifts were quoted in δ as parts per million (ppm) downfield with tetramethylsilane (TMS) as internal reference. Coupling constants, J, are expressed in hertz (Hz). Column

chromatography (CC): silica gel (200 - 300 mesh; Qingdao Makall Group Co., Ltd; Qingdao; China). All reactions were monitored using thinlayer chromatography (TLC) on silica gel plates. On the basis of NMR and HPLC (Thermo Fisher UItiMate 3000, USA) data, all final compounds reported in the manuscript are >95% pure.

4.2. Chemistry (Scheme 1)

4.2.1. General procedure for preparation of compounds 2a-d

A mixture of compound 1 (1 equiv, 10 mmol), malonic acid (1.2 equiv, 12 mmol) and two drops of piperidine in pyridine (25 mL) was refluxed for 4 h and evaporated to remove pyridine. The residue was suspended in H_2O (30 mL) and extracted with EtOAc (2×50 mL) which was further purified by recrystallization to afford 2a-d.

4.2.1.1. (E)-3-(3,4-dimethoxyphenyl)acrylic acid (2a). Yield 82%. m.p. 181-183°C. ESIMS: m/z 208.0600 $[M]^+$, calc. for $C_{11}H_{12}O_4$ (208.21) [27].

4.2.1.2. (E)-3-(3,4,5-trimethoxyphenyl)acrylic acid (2b). Yield 90%. m.p. 126-127°C. ESIMS: m/z 238.6 $[M]^+$, 237.6 $[M-H]^+$, calc. for $C_{12}H_{14}O_5$ (238.24) [28].

4.2.1.3. (E)-3-(benzo[d][1,3]dioxol-5-yl)acrylic acid (2c). Yield 85%. m.p. 242-244 °C. ESIMS: m/z 192.2 $[M]^+$, 408.4 $[2M+Na]^+$, calc. for $C_{10}H_8O_4$ (192.17) [29].

4.2.1.4. (E)-3-(7-methoxybenzo[d][1,3]dioxol-5-yl)acrylic acid (2d). Yield 80%. m.p. 228-229 °C. ESIMS: m/z 221 $[M-H]^+$, calc. for $C_{11}H_{10}O_5$ (222.19) [30].

4.2.2.General procedure for preparation of cinnamoyl chlorides 4a-d

Substituted cinnamoyl chlorides were obtained by refluxing for 5 h the appropriate acid

2a-d (10 mmol) with thionyl chloride (10 ml). After evaporation under reduced pressure, the crude liquid residue was used for subsequent reactions without purification.

4.2.3. General procedure for preparation of compounds 1-3

Hydroxylamine hydrochloride (1.2 equiv, 12 mmol) and sodium acetate (1.2 equiv, 12 mmol) were added to a solution of the aldehyde (1 equiv, 10 mmol) in EtOH (50 ml). The reaction was stirred at 60 ^{o}C for 2 h. After the EtOH was remove evaporated in vacuo, the residue was suspended in DCM (50 ml) and washed with 1 M HCl solution (3×30 ml), H2O (3×30 ml) and brine solution. The organic phase was dried (Na_2SO_4) and then concentrated at reduced pressure. The oximes 1-3 were purified by recrystallization.

4.2.3.1. Picolinaldehyde oxime (1). Yield 100%. m.p. 112-113 ^{o}C. ESIMS: m/z 123.1 $[M+H]^+$, calc. for $C_6H_6N_2O$ (122.12) [31].

4.2.3.2. Furan-2-carbaldehyde oxime (2). Yield 99%. m.p. 88-89 ^{o}C. ESIMS: m/z 112.1 $[M+H]^+$, calc. for $C_5H_5NO_2$ (111.1) [32].

2.2.3.3. Thiophene-2-carbaldehyde oxime (3). Yield 100%. m.p. 130-132 ^{o}C. ESIMS: m/z 128.1 $[M+H]^+$, calc. for C_5H_5NOS (127.16) [33].

4.2.4. General procedure for preparation of compounds 4a-1~4d-3

Oxime (1 equiv, 10 mmol) was resolved in dry DCM (20 ml) and then triethylamine (TEA) (1.2 equiv, 12 mmol) was added drop wise to the solution at 0 ^{o}C and then reaction mixture was stirred for 30 min at 0 ^{o}C. Appropriate acid chloride (1 equiv, 10 mmol) was added to the mixture and then reaction mixture was stirred for 10-20 min at 0 ^{o}C, for 12 h at room

temperature. DCM was evaporated to dryness. The residue was washed with cold ether (5 ml) and hot water and then purified by column chromatography on silica gel eluting with ethyl acetate/ petroleum ether 1:1to 3:1.

4.2.4.1. (E)-picolinaldehyde O-3-(3,4-dimethoxyphenyl)acryloyl oxime (4a-1). White crystal, yield 67%. m.p. 147.0-147.3°C. ^{1}H NMR (500 MHz, $CDCl_3$): δ 3.94 (6H, each 3H, s, H-16,17), 6.45 (1H, d, J=15.91, H-8), 6.90 (1H, d, J=8.30, H-5), 7.11 (1H, d, J=1.94, H-2), 7.18 (1H, dd, J= 1.94, 8.30, H-6), 7.38 (1H, ddd, J=1.00, 1.63, 4.88, H-13), 7.78 (1H, td, J=1.63, 7.91, H-14), 7.84 (1H, d, J=15.91, H-7), 8.17 (1H, d, J=7.91, H-15), 8.54 (1H, s, H-10), 8.68 (1H, dd, J=4.88, H-12). ^{13}C NMR (125 MHz, CDCl3): δ 164.59 (C-9), 156.61 (C-10), 151.59 (C-11), 150.12 (C-3), 149.87 (C-12), 149.27 (C-4), 146.85 (C-7), 136.68 (C-14), 127.13 (C-1), 125.41 (C-13), 123.11 (C-15), 122.10 (C-6), 112.57 (C-8), 111.06 (C-5), 109.77 (C-2), 56.00, 55.92 (C-16, 17). DEPT135: δ 164.31, 153.49, 150.02, 140.61, 129.58 (C), 156.73, 149.86, 146.90, 136.76, 125.49, 122.5, 105.54 (CH), 61.00, 56.20 (CH_3). ESIMS: m/z 313.798 $[M+H]^+$, 336.021 $[M+Na]^+$, 648.812 $[2M+H+Na]^+$, calc. for $C_{17}H_{16}N_2O_4$ (312.32).

4.2.4.2. (E)-furan-2-carbaldehyde O-3-(3,4-dimethoxyphenyl)acryloyl oxime (4a-2). White crystal, yield 53%. m.p. 169.5.1-169.9 °C. ^{1}H NMR (500 MHz, $CDCl_3$): δ 3.96 (6H, each 3H, s, H-15, 16), 6.52 (1H, d, J=15.90, H-8), 6.53 (1H, q, J=1.75, 3.50, H-13), 7.01 (1H, d, J=8.25, H-5), 7.13 (1H, d, J=1.95, H-2), 7.16 (1H, d, J=3.50, H-12), 7.17 (1H, d, J=15.90, H-7), 7.21 (1H, dd, J= 1.95, 8.25, H-6), 7.47(1H, d, J=1.75, H-14), 8.76 (1H, s, H-10). ^{13}C NMR (125 MHz, $CDCl_3$): δ 164.99 (C-9), 158.65 (C-10), 150.82 (C-3), 149.56 (C-11), 149.45 (C-4), 146.30 (C-7), 144.40 (C-14), 130.67 (C-1), 119.81(C-6), 115.23 (C-8), 112.34 (C-13), 111.78

297 (C-5), 110.48 (C-2), 109.49 (C-12), 56.12, 56.07 (C-15, 16). ESIMS: m/z 301.4 [M^+], calc.
298 for $C_{16}H_{15}NO_5$ (301.29).

299 *4.2.4.3. (E)-thiophene-2-carbaldehyde O-3-(3,4-dimethoxyphenyl)acryloyl oxime (4a-3).*
300 White crystal, yield 60%. m.p. 135.8-136.3 °C. ^{1}H NMR (400 MHz, $CDCl_3$): δ 3.95 (6H, each
301 3H, s, H-15, 16), 6.39 (1H, d, J=15.90 Hz, H-8), 6.86(1H, d, J=6.81 Hz, H-5), 7.00 (1H, d,
302 J=1.53 Hz, H-2), 7.19 (1H, dd, J=1.53, 6.81, Hz, H-6), 7.13 (1H, t, J=4.22, 4.49 Hz, H-13),
303 7.55 (1H, d, J=4.49 Hz, H-14), 7.56 (1H, d, J=4.22 Hz, H-12), 7.74 (1H, d, J=15.90 Hz, H-7),
304 8.35 (1H, s, H-10). ^{13}C NMR (100 MHz, $CDCl_3$): δ 165.01 (C-9), 158.88 (C-10), 150.91
305 (C-3), 149.74 (C-4), 146.18 (C-7), 144.32 (C-11), 129.35 (C-1), 127.81 (C-12), 127.15 (C-13),
306 126.20 (C-14), 121.24 (C-6), 114.31 (C-8), 110.54 (C-5), 109.83 (C-2), 56.80, 56.46 (C-15,
307 16). ESIMS: m/z 318.138 [M+H]$^+$, 659.570 [2M+ Na]$^+$, calc. for $C_{16}H_{15}NO_4S$ (317.36).

308 *4.2.4.4. (E)-picolinaldehyde O-3-(3,4,5-trimethoxyphenyl)acryloyl oxime (4b-1).* White
309 crystal, yield 58%. m.p. 121.1-121.3 °C. ^{1}H NMR (500 MHz, $CDCl_3$): δ 3.91 (9H, each 3H, s,
310 H-16, 17, 18), 6.48 (1H, d, J=15.85, H-8), 6.82 (2H, s, H-2, 6), 7.39 (1H, ddd, J=1.10, 2.62,
311 4.94, H-13), 7.80 (1H, td, J=2.62, 7.92, H-14), 7.83 (1H, d, J=15.85, H-7), 8.18 (1H, dm,
312 J=1.10, 7.92, H-15), 8.56 (1H, s, H-10), 8.69 (1H, m, J= 4.94, H-12). ^{13}C NMR (125 MHz,
313 $CDCl_3$): δ 164.31 (C-9), 156.73 (C-10), 153.49 (C-11), 150.02 (C-3, 5), 149.86 (C-12),
314 146.90 (C-7), 140.61 (C-4), 136.76 (C-14), 129.58 (C-1), 125.49 (C-13), 122.15 (C-15),
315 114.20 (C-8), 105.54 (C-2, 6), 61.00 (C-17), 56.20 (C-16, 18). DEPT135: δ 164.31, 153.49,
316 150.02, 140.61, 129.58 (C), 156.73, 149.86, 146.90, 136.76, 125.49, 122.5, 105.54 (CH),
317 61.00, 56.20 (CH_3). ESIMS: m/z 343.1296 [M+H]$^+$, 365.1115 [M+Na]$^+$, calc. for $C_{18}H_{18}N_2O_5$
318 (342.35).

4.2.4.5. (E)-furan-2-carbaldehyde O-3-(3,4,5-trimethoxyphenyl)acryloyl oxime (4b-2). White crystal, yield 59%. m.p. 102.6-102.9 °C. ^{1}H NMR (500 MHz, $CDCl_3$): δ 3.89 (9H, each 3H, s, H-15, 16, 17), 6.43 (1H, q, J=1.95, 3.60, H-13), 6.70 (1H, d, J=15.28, H-8), 6.74 (2H, s, H-2, 6), 6.83 (1H, d, J=3.60, H-12), 7.47(1H, d, J=1.95, H-14), 7.62 (1H, d, J=15.28, H-7), 8.36 (1H, s, H-10). ^{13}C NMR (125 MHz, $CDCl_3$): δ 165.66 (C-9), 159.59 (C-10), 153.43 (C-3, 5), 149.56 (C-11), 146.90 (C-7), 142.39 (C-14), 139.56 (C-4), 129.75 (C-1), 115.56 (C-8), 112.37 (C-13), 109.41 (C-12), 105.10 (C-2, 6),60.97 (C-16), 55.26 (C-15, 17). ESIMS: m/z 332.1207 $[M+H]^+$, 354.1031 $[M+Na]^+$, calc. for $C_{17}H_{17}NO_6$ (331.32).

4.2.4.6. (E)-thiophene-2-carbaldehyde O-3-(3,4,5-trimethoxyphenyl)acryloyl oxime (4b-3). White crystal, yield 51%. m.p. 142.5-142.9 °C. ^{1}H NMR (500 MHz, $CDCl_3$): δ 3.90 (9H, each 3H, s, H-15, 16, 17), 6.48 (1H, d, J=15.85, H-8), 6.82 (2H, s, H-2, 6), 7.13 (1H, q, J=4.91, 5.61 Hz, H-13), 7.56 (1H, d, J=5.61 Hz, H-14), 7.58 (1H, d, J=4.91 Hz, H-12), 7.82 (1H, d, J=15.85, H-7), 8.37 (1H, s, H-10). ^{13}C NMR (125 MHz, $CDCl_3$): δ 165.92 (C-9), 159.34 (C-10), 153.24 (C-3, 5), 146.59 (C-7), 144.32 (C-11), 140.47 (C-4), 129.29 (C-1), 128.03 (C-12), 127.80 (C-13), 125.84 (C-14), 115.28 (C-8), 105.46 (C-2, 6),60.76 (C-16), 56.69 (C-15, 17). ESIMS: m/z 370.3 $[M+Na]^+$, calc. for $C_{17}H_{17}NO_5S$ (347.39).

4.2.4.7. (E)-picolinaldehyde O-3-(benzo[d][1,3]dioxol-5-yl)acryloyl oxime (4c-1). White crystal, yield 52%. m.p. 157.0-157.3 °C. ^{1}H NMR (500 MHz, $CDCl_3$): δ 6.02 (2H, s, H-16), 6.45 (1H, d, J=15.25, H-8), 6.92 (1H, d, J=7.50, H-5), 7.09 (1H, dd, J= 1.84, 7.50, H-6), 7.21 (1H, d, J=1.84, H-2), 7.26 (1H, ddd, J=1.38, 4.75, 5.29, H-13), 7.71 (1H, td, J=5.29, 7.49, H-14), 7.79 (1H, d, J=15.25, H-7), 8.18 (1H, d, J=7.49, H-15), 8.56 (1H, s, H-10), 8.60 (1H, d, J=4.75, H-12). ^{13}C NMR (125 MHz, $CDCl_3$): δ 162.31 (C-9), 155.15 (C-10), 150.54 (C-11),

149.86 (C-12), 149.44 (C-3), 149.16 (C-4), 146.89 (C-7), 136.58 (C-14), 126.53 (C-1), 125.11 (C-13), 123.95 (C-15), 122.77 (C-6), 114.28 (C-8), 109.15 (C-5), 106.88 (C-2), 101.49 (C-16). DEPT135: δ 162.31, 150.54, 149.44, 149.16, 126.53 (C), 155.15, 149.86, 146.89, 136.58, 125.11, 123.95, 122.77, 114.28, 109.15, 106.88 (CH),101.49 (CH_2). ESIMS: m/z 297 $[M+H]^+$, 319 $[M+Na]^+$, calc. for $C_{16}H_{12}N_2O_4$ (296.28).

4.2.4.8. (E)-furan-2-carbaldehyde O-3-(benzo[d][1,3]dioxol-5-yl)acryloyl oxime (4c-2).

White crystal, yield 49%. m.p. 157.8-158.0 °C. ^{1}H NMR (500 MHz, $CDCl_3$): 6.03 (2H, s, H-15), 6.37 (1H, d, J=15.86 Hz, H-8), 6.53 (1H, q, J=1.80, 3.48, H-13), 6.85(1H, d, J=8.02 Hz, H-5), 7.06 (1H, dd, J=1.56, 8.02 Hz, H-6), 7.09 (1H, d, J=1.56 Hz, H-2), 7.17 (1H, dd, J=0.79, 3.48 Hz, H-12), 7.48 (1H, dd, J=0.79, 1.80 Hz, H-14), 7.77 (1H, d, J=15.86 Hz, H-7), 8.36 (1H, s, H-10). ^{13}C NMR (125 MHz, $CDCl_3$): δ 165.22 (C-9), 157.39 (C-10), 149.90 (C-3), 149.41 (C-11), 148.06 (C-4), 146.47 (C-7), 144.41 (C-14), 129.49 (C-1), 119.46(C-6), 115.25 (C-8), 112.35 (C-13), 110.64 (C-5), 109.90 (C-2), 109.15 (C-12), 101.60 (C-15). ESIMS: m/z 308.2 $[M+Na]^+$, calc. for $C_{15}H_{11}NO_5$ (285.25).

4.2.4.9. (E)-thiophene-2-carbaldehyde O-3-(benzo[d][1,3]dioxol-5-yl)acryloyl oxime (4c-3).

White crystal, yield 57%. m.p. 139.6-139.9 °C. ^{1}H NMR (500 MHz, $CDCl_3$): δ 6.02 (2H, s, H-15), 6.40 (1H, d, J=15.57 Hz, H-8), 6.86(1H, d, J=7.76 Hz, H-5), 7.01 (1H, dd, J=1.22, 7.76 Hz, H-6), 7.10 (1H, q, J=4.13, 5.67 Hz, H-13), 7.12 (1H, d, J=1.22 Hz, H-2), 7.52 (1H, d, J=5.67 Hz, H-14), 7.54 (1H, d, J=4.13 Hz, H-12), 7.69 (1H, d, J=15.57 Hz, H-7), 8.36 (1H, s, H-10). ^{13}C NMR (125 MHz, $CDCl_3$): δ 164.75 (C-9), 158.34 (C-10), 149.80 (C-3), 148.84 (C-4), 146.35 (C-7), 143.46 (C-11), 129.31 (C-1), 127.81 (C-12), 127.01 (C-13), 125.06 (C-14), 121.13 (C-6), 114.79 (C-8), 109.95 (C-5), 106.50 (C-2), 101.56 (C-15). ESIMS: m/z

301.1480 [M^+], 323.1103 [M+Na]$^+$, calc. for $C_{15}H_{11}NO_4S$ (301.32).

4.2.4.10. (E)-picolinaldehyde O-3-(7-methoxybenzo[d][1,3]dioxol-5-yl)acryloyl oxime (4d-1). White crystal, yield 58%. m.p. 186.3-186.6 ˚C. ^{1}H NMR (500 MHz, $CDCl_3$): δ 3.95 (3H, s, H-17), 6.04 (2H, s, H-16), 6.42 (1H, d, J=15.89, H-8), 6.77 (1H, d, J=1.25, H-6), 6.82 (1H, d, J=1.25, H-2), 7.39 (1H, m, J= 1.74, 6.89, H-13), 7.79 (1H, td, J=1.40, 7.92, H-14), 7.77 (1H, d, J=15.89, H-7), 8.17 (1H, d, J=7.92, H-15), 8.55 (1H, s, H-10), 8.69 (1H, dd, J=4.42, H-12). ^{13}C NMR (125 MHz, CDCl3): δ 164.46 (C-9), 156.60 (C-10), 150.04 (C-11), 149.80 (C-12), 149.46 (C-5), 146.71 (C-7), 143.75 (C-3), 137.88 (C-4), 136.82 (C-14), 128.95 (C-1), 125.48 (C-13), 122.17 (C-15), 113.39 (C-8), 109.69 (C-6), 101.49 (C-2), 102.12(C-16), 56.67 (C-17). DEPT135: δ 164.46, 150.04, 149.46, 143.75, 137.88, 128.95 (C), 156.60, 149.80, 146.71, 136.82, 125.48, 122.17, 113.39, 109.69, 101.49 (CH), 102.12 (CH_2), 56.67 (CH_3). ESIMS: m/z 327.0987 [M+H]$^+$, 349.0807 [M+Na]$^+$, calc. for $C_{17}H_{14}N_2O_5$ (326.3).

4.2.4.11. (E)-furan-2-carbaldehyde O-3-(7-methoxybenzo[d][1,3]dioxol-5-yl)acryloyl oxime (4d-2). White crystal, yield 64%. m.p. 122.5-122.8 ˚C. ^{1}H NMR (500 MHz, $CDCl_3$): δ 3.94 (3H, s, H-16), 6.03 (2H, s, H-15), 6.39 (1H, d, J=15.85 Hz, H-8), 6.92 (1H, d, J=1.36 Hz, H-6), 7.01 (1H, d, J=1.36 Hz, H-2), 6.52 (1H, q, J=1.75, 3.45 Hz, H-13), 7.17(1H, dd, J=0.80, 3.45 Hz, H-12), 7.47 (1H, d, J=0.80, 1.75, H-16), 7.75 (1H, d, J=15.85 Hz, H-7), 8.36 (1H, s, H-10). ^{13}C NMR (125 MHz, CDCl3): δ 165.00 (C-9), 159.37 (C-10), 150.49 (C-5), 149.33 (C-11), 146.58 (C-7), 144.17 (C-14), 143.24 (C-3), 136.80 (C-4), 128.75 (C-1), 115.18 (C-8), 112.33 (C-13), 109.92(C-6),109.56 (C-12), 101.60 (C-15), 101.45 (C-2), 56.44 (C-16). ESIMS: m/z 338.3423 [M+Na]$^+$, calc. for $C_{16}H_{13}NO_6$ (315.28).

4.2.4.12. (E)-thiophene-2-carbaldehyde O-3-(7-methoxybenzo[d][1,3]dioxol-5-yl)acryloyl

oxime (4d-3). White crystal, yield 61%. m.p. 132.6-133.2 °C. ^{1}H NMR (500 MHz, $CDCl_3$): δ 3.92 (3H, s, H-16), 6.00 (2H, s, H-15), 6.67(1H, d, J=1.18 Hz, H-2), 6.74 (1H, d, J=15.28 Hz, H-8), 6.75(1H, d, J=1.18 Hz, H-6), 6.93 (1H, d, J=3.97 Hz, H-12), 7.17 (1H, q, J=3.97, 4.72 Hz, H-13), 7.19 (1H, d, J=4.72 Hz, H-14), 7.53 (1H, d, J=15.28 Hz, H-7), 8.36 (1H, s, H-10). ^{13}C NMR (125 MHz, $CDCl_3$): δ 164.36 (C-9), 160.04 (C-10), 149.29 (C-5), 146.41 (C-7), 143.61 (C-3),142.09 (C-11), 136.58 (C-4), 130.38 (C-1), 127.80 (C-12), 127.59 (C-13), 126.07 (C-14), 115.93 (C-8), 109.04 (C-6), 101.82 (C-15), 100.70 (C-2), 56.69 (C-16). DEPT135: δ 164.36, 149.29, 143.61, 136.58, 130.38 (C), 160.04, 146.41, 142.09, 127.80, 127.59, 126.07, 115.93, 109.04, 100.70 (CH), 101.82 (CH_2), 56.69 (CH_3). ESIMS: m/z 332.4 $[M+H]^+$, 354 $[M+Na]^+$, calc. for $C_{16}H_{13}NO_5S$ (331.34).

4.3. Molecular docking studies

The ligand study was carried out by HyperChem software, a sophisticated molecular modeling environment that uniting with quantum chemical calculations, dynamics, and molecular mechanics [34]. Three-dimensional structures were constructed and optimized for all the molecules, and then QSAR descriptors were studied, which is a powerful lead optimization tool that can quantitatively relate variations in biological activity to changes in molecular properties.

In our previous studies, niranthin, nirtetralin, nirtetralin A and nirtetralin B from *Phyllanthus niruri L.* were confirmed to possess anti-HBV activity [10-12]. Then we investigated the potential anti-HBV targets of the anti-HBV constituents with reverse docking approach using fifteen HBV related proteins and RNA including human leukocyte antigen

406 HLA-A*02:03 (PDB ID: 3OX8), human leukocyte antigen HLAA*02:06 (PDB ID: 3OXR),
407 human leukocyte antigen HLA-A*02:07 (PDB ID: 3OXS), hepatitis B virus preS1 protein
408 (PDB ID: 3ZHF), hepatitis B virus preS2 surface antigen (PDB ID: 1WZ4), human hepatitis
409 B virus surface antigen HzKR127 (PDB ID: 2EH8), human hepatitis B virus e-antigen (PDB
410 ID: 3V6F, 3V6Z), Hepatitis B X-interacting protein HBXIP (PDB ID: 3MS6, 4WZR,
411 4WZW), HBV RNA polymerase (PDB ID: 2HN7), and human hepatitis **B** virus encapsidation
412 signal (PDB ID: 2IXY, 2K5Z). HLA-A protein (PDB ID: 3OX8) showed the best reverse
413 docking result and was chosen as molecular target for further docking study.
414 The molecular docking study was performed using MOE 2008.10 to understand the
415 ligand-protein interactions in detail. The target compounds were built using the builder
416 interface of the MOE program and subjected to energy minimization. The crystal structure of
417 human leukocyte antigen (HLA-A) protein (PDB ID: 3OX8) was retrieved from Protein Data
418 Bank (http://www.rcsb.org/pdb/home/home.do) [35]. The edited crystal structure after
419 removing water molecules was imported into MOE and chain A was considered for docking
420 process as the protein is a dimer consisting of A and B chains. The structure is protonated,
421 polar hydrogens were added and energy minimization was carried out till the gradient
422 convergence 0.05 kcal/mol was reached to get the stabilized conformation. The active site was
423 correlated with 'Site Finder' module of MOE to define the docking site for the ligands.
424 Docking procedure was followed using the standard protocol implemented in MOE 2008.10
425 and the geometry of resulting complexes was studied using the MOE's Pose Viewer utility.

426 4.4. Pharmacology

427 *4.4.1. Cells and Cell culture*

428 HepG2.2.15 (clonal cells derived fromhuman hepatoma cell line G2) cells were provided
429 by the Chinese Academy of Medical Sciences (P.R. China) and maintained in MEM medium
430 supplemented with 10% fetal bovine serum and 380 μg/ml of G418, 50 u/ml of kanamycin,
431 and 0.03% L-glutamine at 37 ^{o}C in a 5% CO_2 atmosphere with 100% humidity.

432 *4.4.2. Drug treatment*

433 HepG 2.2.15 cells were seeded at a density of 1×10^5 cells/ml (200 μl/well) in 96-well plates
434 and maintained at 37 ^{o}C for 24 h prior to extract addition, followed by treatment with various
435 concentrations of drugs. Lamivudine (3TC) was served as the positive control. Cells were
436 refed with drug-containing fresh medium every 3 d for up to 9 d in time-dependent
437 experiment. Medium was taken at third day of treatment (T3), the sixth day of treatment (T6)
438 and the ninth day of treatment (T9), and stored at -20 ^{o}C until analysis. The IC_{50} and selected
439 index (SI) of each compound were calculated, respectively.

440 *4.4.3. Cell toxicity*

441 Logarithmically growing cells were seeded in 96-well culture plates at a density of 1×10^5
442 cells/ml (200 μl/well). They were cultured for 24 h and then treated with various
443 concentrations of drugs. OD values were read at 450 nm after 9days and the percent of cell
444 death was calculated and the cells were refed with drug-containing fresh medium every 3 d
445 for up to 9 d. After drug treatment, the cytotoxicity was measured using the MTT assay [36,
446 37].

447 *4.4.4. Determination of HBsAg and HBeAg*

448 The levels of HBV surface antigen (HBsAg) and HBV e antigen (HBeAg) were
449 simultaneously detected using ELISA kits (Rongsheng Biotechnology Co. Ltd, Shanghai,
450 China) according to the manufacturer's instructions.

451 *4.4.5. Determination of HBV replication*

452 Inhibitory activity against HBV was determined by a real-time fluorescence quantitative PCR
453 (FQ-PCR) according to our previous description [11]. Briefly, 2.0 µl HBV DNA was
454 amplified in a 25 mL mixture containing 12.5 µl 2 × SYBR Green Master (ROX) and 2
455 primers specific for HBV: a forward primer (5′-AAC CAT TGA AGC AAT CAC TAG AC-3′)
456 and a reverse primer (5′- ATC TAT GGT GGC TGC TCG AAC TA -3′). The thermal program
457 comprised of an initial denaturation at 95 ^{o}C for 10 min followed by 40 amplification cycles
458 with each of the two following steps: 95 ^{o}C for 15 s and 60 ^{o}C for 1 min.

459 **Acknowledgements**

460 This work was financially supported by the national natural science foundation of China
461 (No. 81060261), natural science foundation of Guangxi province, China, (No. 2011jjD20002),
462 and science research and technology development foundation of Guagnxi province, China
463 (No.11107009-3-5)

464 **References**

465 [1] N. Gitilin, HepatitisB: diagnosis, prevention and treatment. Clin. Biochem. 43 (1997)

1500-1506.

[2] M. Rizzetto, A. Ciancio, Chronic HBV-related liver disease. Mol. Aspects Med. 29 (2008) 72-84.

[3] D. Lavanchy, Hepatitis B virus epidemiology, disease burden, treatment, and current and emerging prevention and control measures. J. Viral Hepat. 11 (2004) 97-107.

[4] K. Sato, M. Mori, Current and Novel Therapies for Hepatitis B Virus Infection. Mini-Rev. Med. Chem. 10 (2010) 20-31.

[5] C.X. Ying, Y. Li, C.H. Leung, M.D. Robek, Y.C. Cheng, Unique antiviral mechanism discovered in anti-hepatitis B virus research with a natural product analogue. Proc. Natl. Acad. Sci. U.S.A. 104 (2007) 8526-8531.

[6] L.M. Gao, Y.X. Han, Y.P. Wang, Y.H. Li, Y.Q. Shan, X. Li, Z.G. Peng, C.W. Bi, T. Zhang, N.N. Du, J.D. Jiang, D.Q. Song, Design and Synthesis of Oxymatrine Analogues Overcoming Drug Resistance in Hepatitis B Virus through Targeting Host Heat Stress Cognate 70. J. Med. Chem. 54 (2011) 869-876.

[7] I.T. Crosby, D.G. Bourke, E.D. Jones, T.P. Jeynes, S. Cox, J.A.V. Coates, A.D. Robertson, Antiviral agents 3. Discovery of a novel small molecule non-nucleoside inhibitor of Hepatitis B Virus (HBV). Bioorg. Med. Chem. Lett. 21 (2011) 1644-1648.

[8] N.N. Du, X. Li, Y.P. Wang, F. Liu, Y.X. Liu, C.X. Li, Z.G. Peng, L.M. Gao, J.D. Jiang, D.Q. Song, Synthesis, structure-activity relationship and biological evaluation of novel N-substituted matrinic acid derivatives as host heat-stress cognate 70 (Hsc70) down-regulators. Bioorg. Med. Chem. Lett. 21 (2011) 4732-4735.

[9] L.J. Wang, C.A. Geng, Y.B. Ma, X.Y. Huang, J. Luo, H. Chen, R.H. Guo, X.M. Zhang, J.J.

Chen. Synthesis, structure – activity relationships and biological evaluation of caudatin derivatives as novel anti-hepatitis B virus agents. Bioorgan. Med. Chem. 20 (2012) 2877-2888.

[10] W.X. Wei, X.R. Li, K.W. Wang, Z.W. Zheng, M. Zhou, Lignans with Anti-Hepatitis B Virus Activities from Phyllanthus niruri L. Phytother. Res. 26 (2012) 964-968.

[11] S. Liu, W.X. Wei, K.C. Shi, X. Cao, M. Zhou, Z.P. Liu, In vitro and in vivo anti-hepatitis B virus activities of the lignan niranthin isolated from Phyllanthus niruri L. J. Ethnopharmacol. 155 (2014) 1061-1067.

[12] S. Liu, W.X. Wei, Y.B. Li, X. Lin, K.C. Shi, X. Cao, M. Zhou, In vitro and in vivo anti-hepatitis B virus activities of the lignan nirtetralin B isolated from Phyllanthus niruri L. J. Ethnopharmacol. 157 (2014) 62-68.

[13] C. Viegas-Junior, A. Danuello, V.D. Bolzani, E.J. Barreir, C.A.M. Fraga, Molecular hybridization: A useful tool in the design of new drug prototypes. Curr. Med. Chem. 14 (2007) 1829-1852.

[14] H. Chen, Y.B. Ma, X.Y. Huang, C.A. Geng, Y. Zhao, L.J. Wang, R.H. Guo, W.J. Liang, X.M. Zhang, J.J. Chen, Synthesis, structure – activity relationships and biological evaluation of dehydroandrographolide and andrographolide derivatives as novel anti-hepatitis B virus agents. Bioorg. Med. Chem. Lett. 24 (2014) 2353-2359.

[15] Z.R. Wu, L.F. Zheng, Y. Li, F. Su, X.X. Yue, W. Tang, X.Y. Ma, J.Y. Nie, H.Y. Li, Synthesis and structure–activity relationships and effects of phenylpropanoid amides of octopamine and dopamine on tyrosinase inhibition and antioxidation. Food Chem. 134 (2012) 1128-1131.

[16] S.N. Kim, J.Y. Lee, H.J. Kim, C.G. Shin, H. Parka, Y.S. Lee, Synthesis and HIV-1 Integrase Inhibitory Activities of Caffeoylglucosides. *Bioorg.* Med. Chem. Lett. 10 (2000) 1879-1882.

[17] P. Panda, M. Appalashetti, M. Natarajan, C.P. Mary, S.S. Venkatraman, Z.M.A. Judeh, Synthesis and antiproliferative activity of helonioside A,3',4',6'-tri-O-feruloylsucrose, lapathoside C and their analogs. Eur. J. Med. Chem. 58 (2012) 418-430.

[18] P. Panda, M. Appalashetti, M. Natarajan, M.B. Chan-Park, S.S. Venkatraman, Z.M.A. Judeh, Judeh. Synthesis and antitumor activity of lapathoside D and its analogs. Eur. J. Med. Chem. 53 (2012) 1-12.

[19] F. Zhang, G. Wang, A review of non-nucleoside anti-hepatitis B virus agents. Eur. J. Med. Chem. 75 (2014) 267-281.

[20] Y.K. Zhang, H.Y. Zhong, Z.L. Lv, M.F. Zhang, T. Zhang, Q.S. Li, K. Li, Anti-hepatitis B virus and anti-cancer activities of novel isoflavone analogs. Eur. J. Med. Chem. 62 (2013) 158-167.

[21] L. Roux, S. Priet, N. Payrot, C. Weck, M. Fournier, F. Zoulim, J. Balzarini, B. Canard, K. Alvarez, Ester prodrugs of acyclic nucleoside thiophosphonates compared to phosphonates: Synthesis, antiviral activity and decomposition study. Eur. J. Med. Chem. 63 (2013) 869-881.

[22] F.D. Santos, P. Abreu, H.C. Castro, I.C.P.P. Paixao, C.C. Cirne-Santos, V. Giongo, J.E. Barbosa, B.R. Simonetti, V. Garrido, D.C. Bou-Habib, D.D. Silva, P.N. Batalha, J.R. Temerozo, T.M. Souza, C.M. Nogueira, A.C. Cunha, C.R. Rodrigues, V.F. Ferreira, M.C.B.V. de Souza, Synthesis, antiviral activity and molecular modeling of oxoquinoline

532 derivatives. Bioorgan. Med. Chem. 17 (2009) 5476-5481.

533 [23] K.R. Babu, V.K. Rao, Y.N. Kumar, K. Polireddy, K.V. Subbaiah, M. Bhaskar, V.

534 Lokanatha, C.N. Raju. Identification of substituted [3, 2-a] pyrimidines as selective

535 antiviral agents: Molecular modeling study. Antivir. Res. 95 (2012) 118-127.

536 [24] V.V. Quan, C. Trenerry, S. Rochfort, J. Wadeson, C. Leyton, A,B. Hughes, Synthesis and

537 anti-inflammatory activity of aromatic glucosinolates. Bioorgan. Med. Chem. 21 (2013)

538 5945-5954.

539 [25] H.B. Zou, H. Wu, X.N. Zhang, Y. Zhao, S. Joachim, Y.J. Lou, Y.P. Yu, Synthesis,

540 biological evaluation, and structure-activity relationship study of novel cytotoxic

541 aza-caffeic acid derivatives. Bioorgan. Med. Chem. 18 (2010) 6351-6359.

542 [26] A. Karakurt, A.A.B.S. Mehmet,Ü. Çalıs, S.Dalkara, Synthesis of some novel

543 1-(2-naphthyl)-2-(imidazol-1-yl)ethanone oxime ester derivatives and evaluation of their

544 anticonvulsant activity. Eur. J. Med. Chem. 57 (2012) 275-282.

545 [27] Brittelli, R. David, Phosphite-mediated in situ carboxyvinylation: a new general acrylic

546 acid synthesis. J. Org. Chem. 46 (1981) 2514-2520.

547 [28] M.W. Klohs, M.D. Draper, F. Keller, Alkaloids of Rauwolfia serpentina. III.

548 Rescinnamine, a new hypotensive and sedative principle. J. Am. Chem. Soc. 76 (1954)

549 2843.

550 [29] M.L. Salum, C.J. Robles, R. Erra-Balsells, Photoisomerization of Ionic Liquid

551 Ammonium Cinnamates: One-Pot Synthesis-Isolation of Z-Cinnamic Acids. Org. Lett.

552 12 (2010) 4808-4811.

553 [30] A.H. Salway, Synthesis of Substances Allied to Cotarnine. J. Chem. Soc. Transactions.

95 (1909) 1204-1220.

[31] E.J. Poziomek, B.E.J. Hackley, G.M. Steinberg, Pyridinium aldoximes. J. Org. Chem. 23 (1958) 714-717.

[32] J. Nidhi, K. Anil, S.M.S. Chauhan, Metalloporphyrin and heteropoly acid catalyzed oxidation of CNOH bonds in an ionic liquid: biomimetic models of nitric oxide synthase. Tetrahedron Lett. 46 (2005) 2599-2602.

[33] L. Fernando, D.L.C. Pilar, E. Eva, G.C. Araceli, D.L.H. Antonio, L.A. Vicente, Synthesis and Properties of Isoxazolo[60]fullerene-Donor Dyads. J. Org. Chem. 65 (2000) 8675-8684.

[34] S. Dastmalchi, M. Hamzeh-Mivehroud, T. Ghafourian, H. Hamzeiy, Molecular modeling of histamine H3 receptor and QSAR studies on arylbenzofuran derived H3 antagonists. J. Mol. Graph. Model. 26 (2008) 834-844.

[35] J.X. Liu, Y. Kenneth, E.C.R. Chen, Structural insights into the binding of hepatitis B virus core peptide to HLA-A2 alleles: Towards designing better vaccines. Eur. J. Immunol. 41 (2011) 2097-2106.

[36] M. Ferrari, M.C. Fornasiero, A.M. Isetta, MTT colorimetric assay for testing macrophage cytotoxic activity in vitro. J. Immunol. Methods. 131 (1990) 165-172.

[37] Y.Q. Han, Z.M. Huang, X.B. Yang, H.Z. Liu, G.X. Wu, In vivo and in vitro anti-hepatitis B virus activity of total phenolics from Oenanthe javanica. J. Ethnopharmacol. 118 (2008) 148-153.

Legend of figures

Scheme 1. Synthetic route to the series of compounds. Reagents and conditions: (a) $CH_2(COOH)_2$, piperidine, C_5H_5N, reflux, 4h, 80-90%; (b) $SOCl_2$, CH_2Cl_2, reflux, 5h, 95%; (c) H_2NOH-HCl, AcONa, EtOH, 60^oC, 1h, 98%; (d) Et_3N, CH_2Cl_2, rt, 12h, 50-70%.

Table 1. Molecular descriptors of derivatives from QSAR study.

Table 2. Docking score and bond interactions of synthesized compounds.

Table 3. Anti-HBV activity and cytotoxicity of the phenylpropanoid derivatives in vitro.

Figure 1. Binding mode of 4c-1 into the binding site of HLA-A. The hydrogen bond formed colored in green.

Figure 2. Binding mode of 4d-1 into the binding site of HLA-A. The hydrogen bond formed colored in green.

Figure 3. Binding mode of 4d-2 into the binding site of HLA-A. The hydrogen bond formed colored in green.

Figure 4. Inhibitory effect of the phenylpropanoid derivatives on secretion of HBsAg (A) and HBeAg (B) in the HepG2.2.15 cell line. Data were expressed as mean ± S.D. (n = 3).

Table 2. Docking score and bond interactions of synthesized compounds.

Ligand	S-score (kcal/mol)	No. of H-bonds	Distance (A)	Amino acid involved	Molecular structure
3TC	-10.7074	2	2.03	TYR 27	O of -OH
			2.29	TYR 27	O of -COC-
4a-1	-15.0037	2	1.77	TYR 27	O of -ON
			2.77	TYR 27	N of pyridine
4a-2	-14.1510	0	-	-	-
4a-3	-14.1436	1	2.67	TYR 27	O of -ON
4b-1	-16.5849	2	2.63	TYR 27	O of -ON
			3.39	TYR 27	N of pyridine
4b-2	-16.4346	1	2.98	TYR 27	O of -ON
4b-3	-16.4019	1	2.99	TYR 27	O of -ON
4c-1	-18.3979	2	2.02	TYR 27	O of -ON
			3.49	TYR 27	N of pyridine
4c-2	-12.5508	1	1.89	TYR 27	O of -ON
4c-3	-12.4670	1	1.90	TYR 27	O of -ON
4d-1	-16.6093	1	3.03	TYR 27	O of -ON
4d-2	-16.5985	1	2.87	TYR 27	O of -ON
4d-3	-14.8563	1	2.86	TYR 27	O of -ON

Table 3. Anti-HBV activity and cytotoxicity of the phenylpropanoid derivatives in vitro.

Compd	CC_{50}[b] (μM)	HBsAg[c]		HBeAg[d]		DNA replication	
		IC_{50}[e] (μM)	SI[f]	IC_{50}[e] (μM)	SI[f]	IC_{50}[e] (μM)	SI[f]
1a	＞1500	-[g]	-	-	-	ND	ND
1b	＞1500	-	-	-	-	ND	ND
1c	1289.31	-	-	-	-	ND	ND
1d	1075.75	-	-	-	-	ND	ND
2a	534.66	＞600	＜0.89	＞600	＜0.89	ND	ND
2b	834.13	＞600	＜1.39	＞600	＜1.39	ND	ND
2c	503.46	433.15	1.16	526.25	0.96	ND	ND
2d	667.25	410.96	1.62	476.75	1.40	ND	ND
1	402.02	387.17	1.04	469.11	0.86	ND	ND
2	475.21	479.80	1.01	519.47	0.91	ND	ND
3	562.19	353.56	1.59	431.23	1.30	ND	ND
4a-1	545.16	151.87	3.59	161.74	3.37	ND	ND
4a-2	624.24	191.26	3.26	201.65	3.10	ND	ND
4a-3	574.33	228.67	2.51	377.87	1.52	ND	ND
4b-1	787.32	142.67	5.52	150.08	5.25	ND	ND
4b-2	1049.90	173.31	6.06	189.67	5.54	ND	ND
4b-3	857.37	196.62	4.36	209.22	4.10	ND	ND
4c-1	253.11	14.18	17.85	6.20	40.82	23.43	10.80
4c-2	479.62	64.60	7.42	81.83	5.86	-	-
4c-3	265.78	75.75	3.51	117.67	2.26	ND	ND
4d-1	644.93	62.79	10.27	72.91	8.85	95.04	6.78
4d-2	819.58	63.51	12.90	75.26	10.89	139.73	5.87
4d-3	676.60	74.37	9.10	104.52	6.47	-	-
3TC[h]	568.25	234.70	2.42	267.16	2.13	6.86	82.84

a Values are means determined from at least two experiments.
b CC_{50} is 50% cytotoxicity concentration in HepG2 2.2.15 cells.
c HBsAg: hepatitis B surface antigen.
d HBeAg, hepatitis B e antigen.
e IC_{50} is 50% inhibitory concentration.
f SI (selectivity index) = CC_{50}/IC_{50}.
g No SI can be obtained.
h Lamivudine (3TC) as the positive control.
g Not determined.

Table 1. Molecular descriptors of derivatives from QSAR study.

Ligand	Molecular weight (Da)	LogP	Molar refractivity (A^{o3})	Surface area (A^{o2})	Volume (A^{o3})	Hydration energy (Kcal/mol)	Polarizability (A^{o3})
3TC	229.25	-0.55	55.14	525.55	606.87	48.20	21.71
4a-1	312.32	0.61	93.01	704.41	912.63	43.90	33.13
4a-2	317.36	-1.08	90.78	729.25	898.62	47.75	32.20
4a-3	317.36	-0.81	93.60	709.11	904.30	44.77	33.36
4b-1	342.35	-0.38	99.38	757.97	974.66	43.66	35.61
4b-2	331.32	-2.14	93.53	756.01	944.36	43.13	33.47
4b-3	347.39	-1.80	99.98	762.65	966.33	44.54	35.84
4c-1	296.28	0.80	85.85	715.19	837.91	41.55	30.52
4c-2	285.25	-0.96	80.00	713.15	807.65	41.03	28.39
4c-3	301.32	-0.62	86.44	719.87	829.56	42.42	30.76
4d-1	326.3	-0.19	92.22	761.65	907.50	40.43	33.00
4d-2	315.28	-1.95	86.37	759.71	877.24	39.90	30.86
4d-3	331.34	-1.61	92.82	766.32	899.14	41.31	33.23

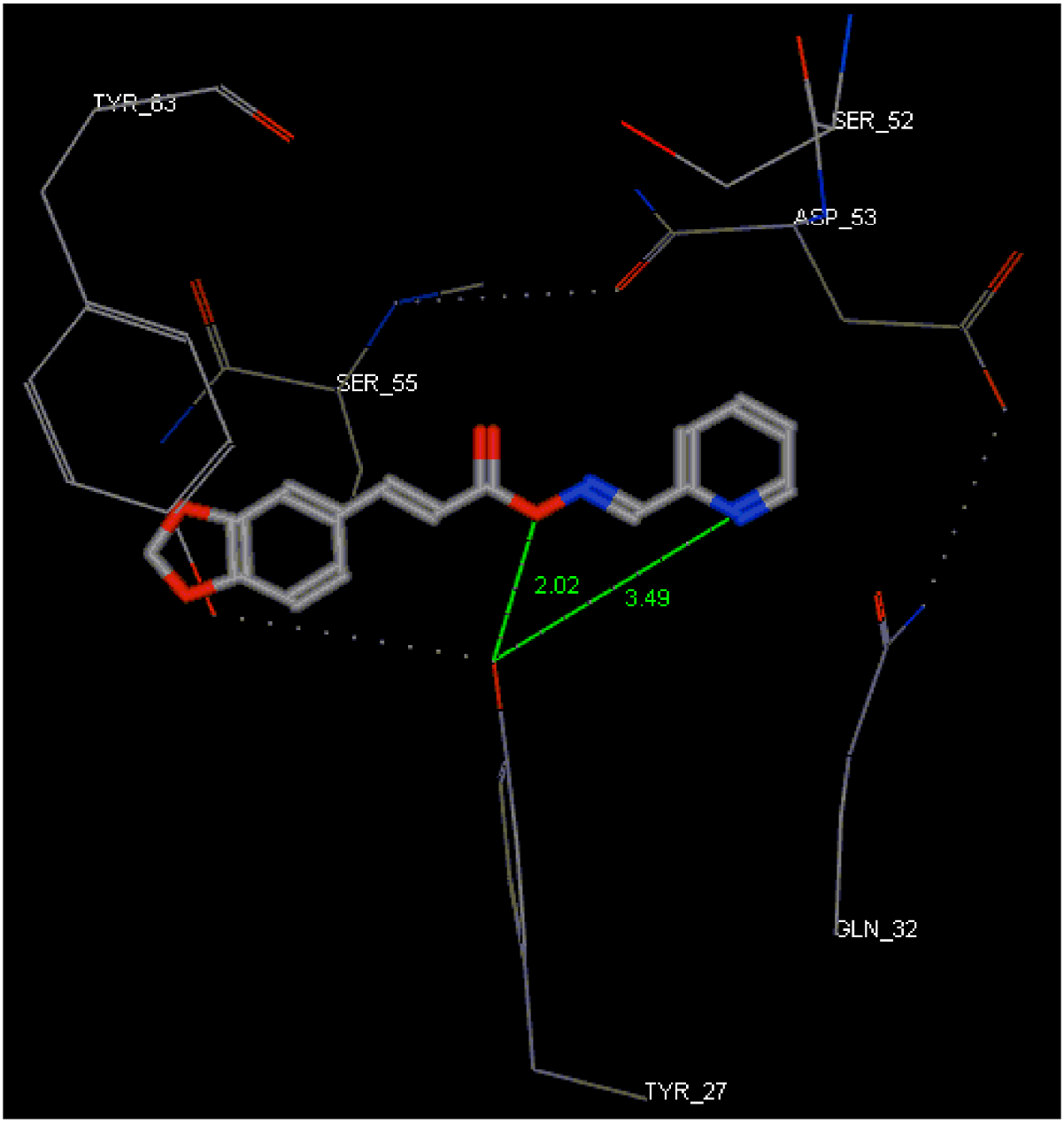

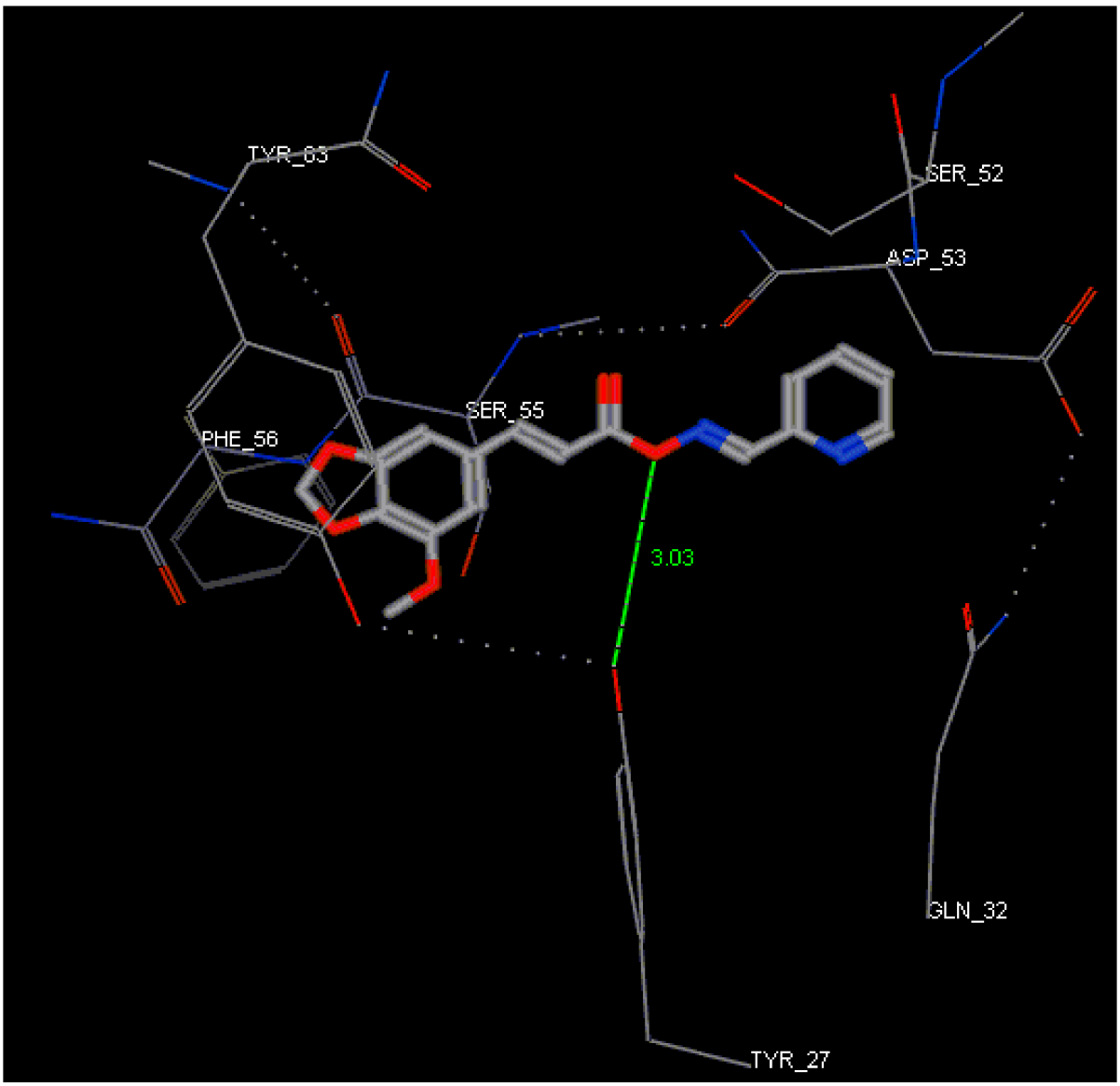

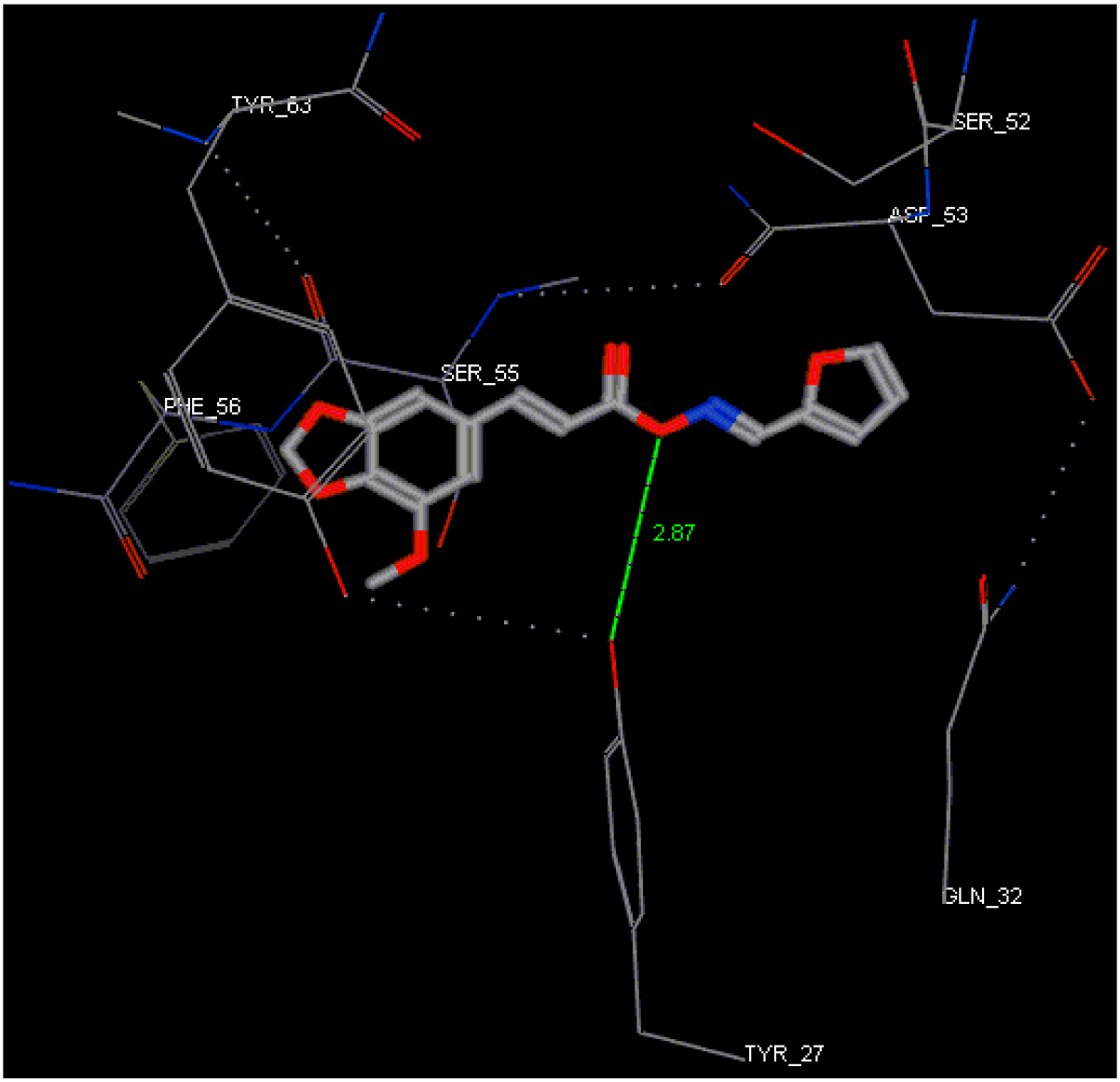

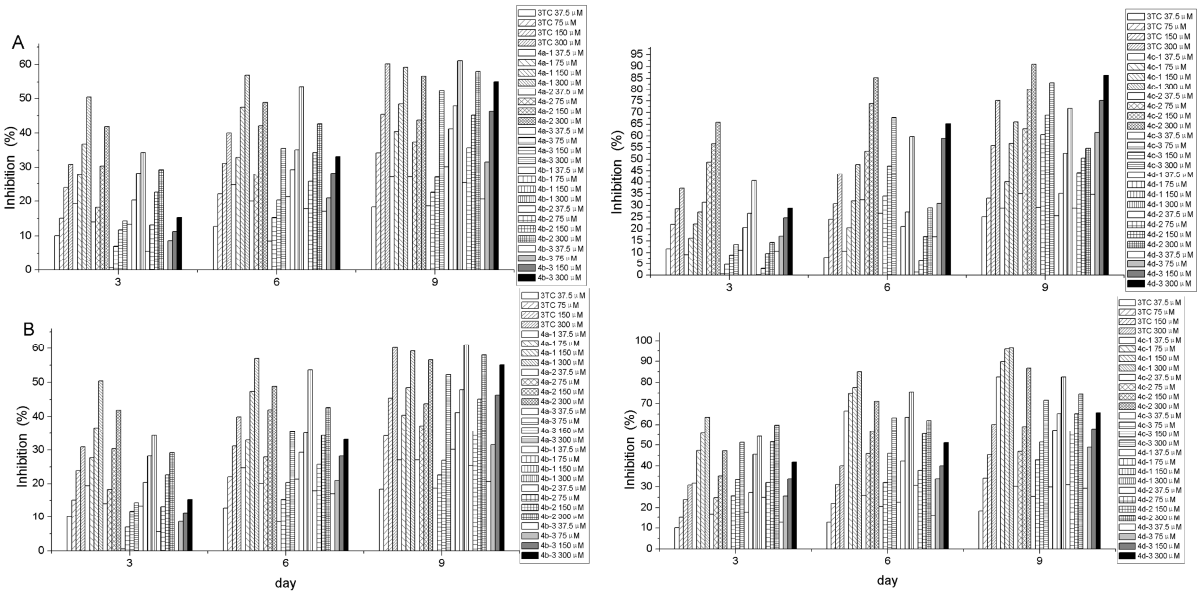

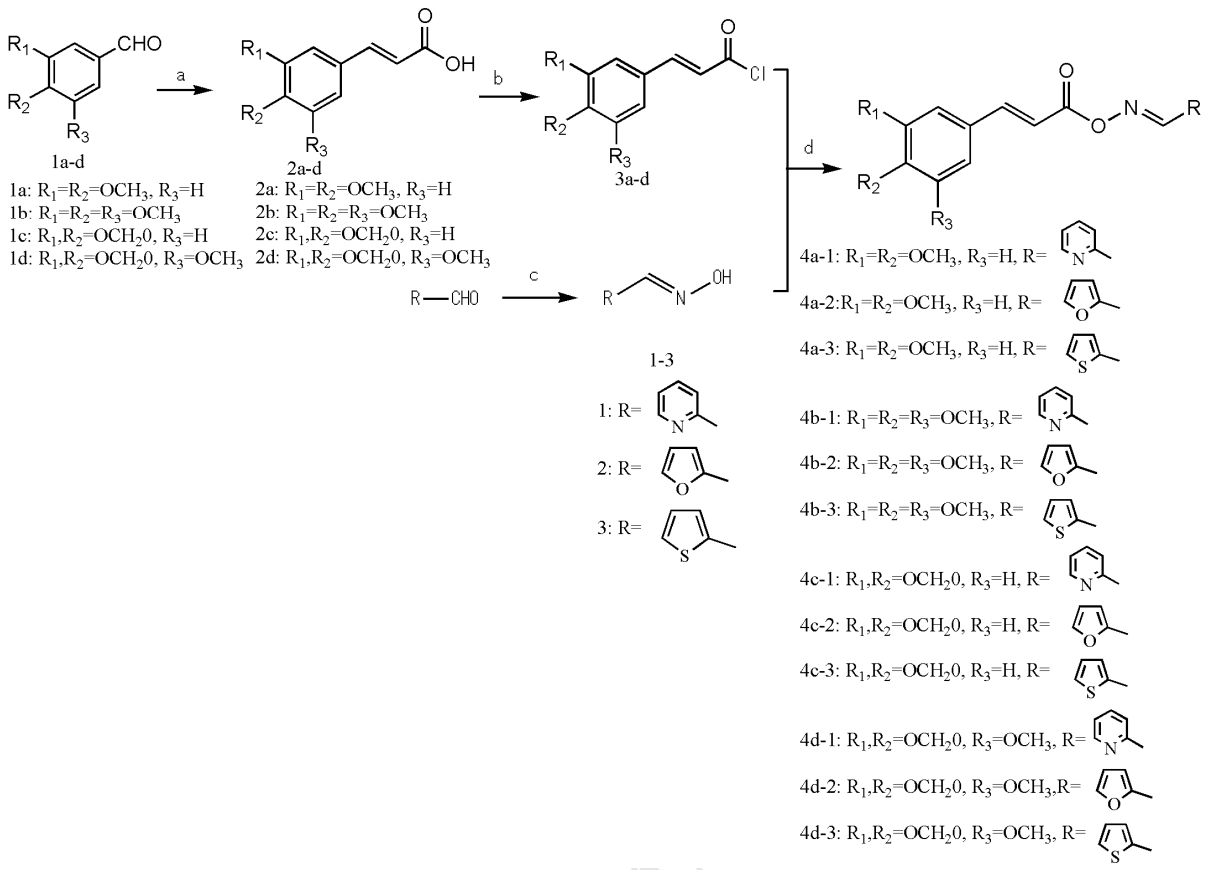

Highlights

- A series of phenylpropanoid derivatives were designed and synthesized based on our previous studies.
- The human HBV-transfected liver cell line HepG2.2.15 was used in vitro assay.
- The structure-activity relationships of the derivatives had been discussed in the paper.
- Docking study was carried out to explore molecular target for activity using MOE.
- Compound 4c-1exhibited the most potent anti-HBV activities.

Design, synthesis, biological evaluation and molecular docking studies of phenylpropanoid derivatives as potent anti-hepatitis B virus agents

Sheng Liu[1], Wanxing Wei *[1], Yubin Li[2], Xu Liu[1], Xiaoji Cao[3], Kechan Lei[1], Min Zhou[1]

[1]Department of Chemistry, Guangxi University, Nanning, 530004, P. R. China

[2]School of Chemistry and Chemical Engineering, Sun Yat-Sen University, Guangzhou 510275, P. R. China

[3]Center of Analysis and Testing, Zhejiang University of Industry, Hangzhou, 310014, P. R. China

*Corresponding author. Tel.: +86 7713272601. fax +86 7713272601. E-mail: wxwei@gxu.edu.cn (W. Wei)

List of supporting information

Figures

Tables

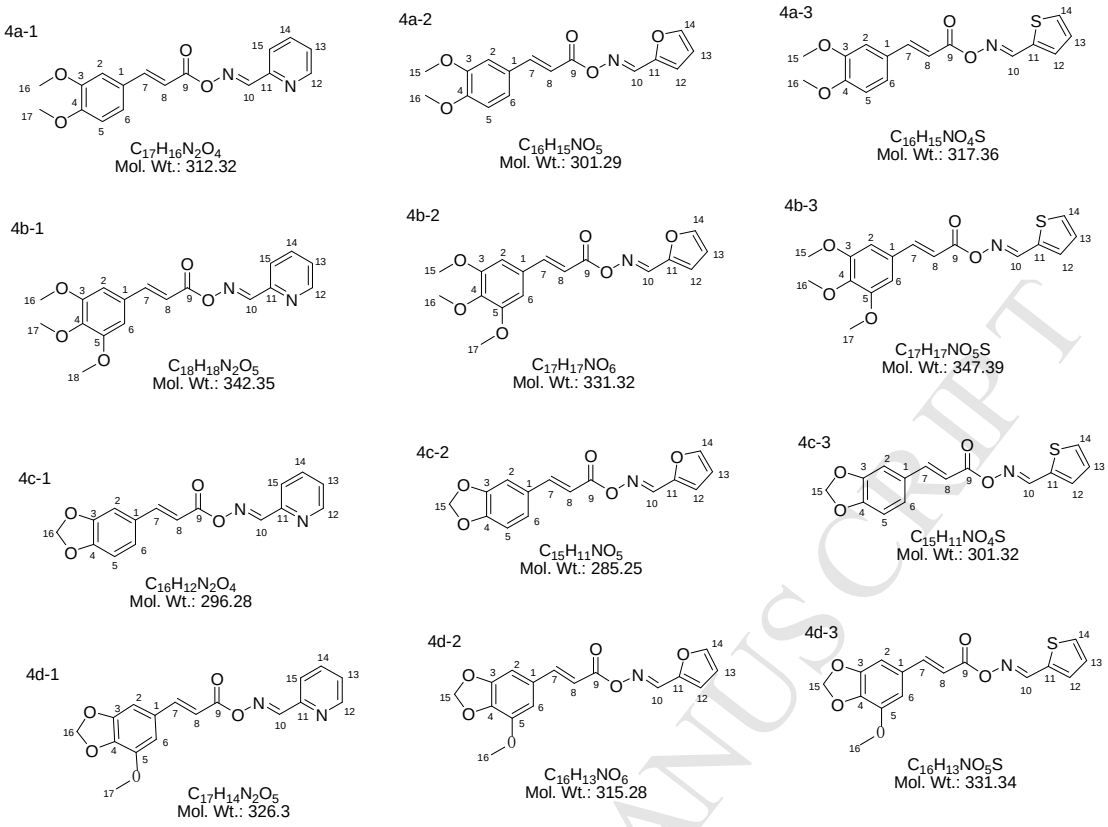

Figure 1. Chemical structure of phenylpropanoid derivatives

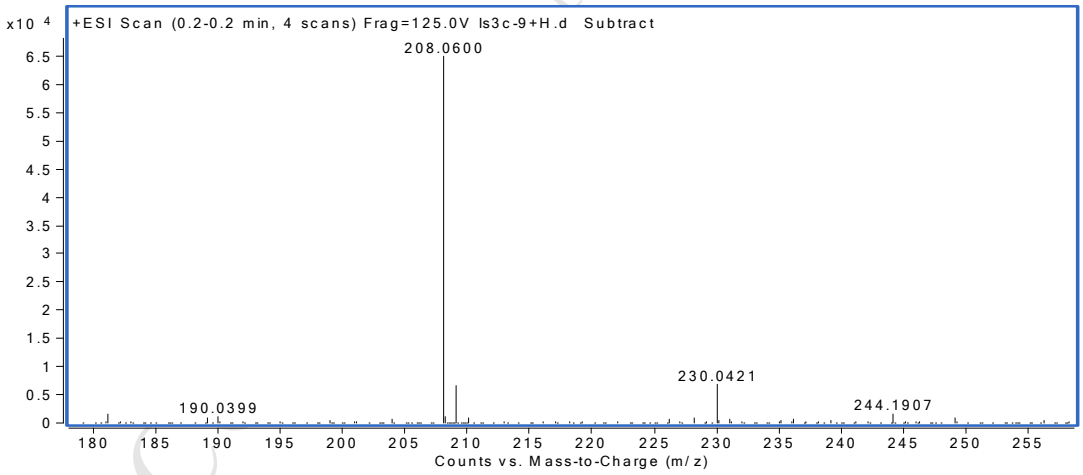

Figure 2. MS spectrum of 2a

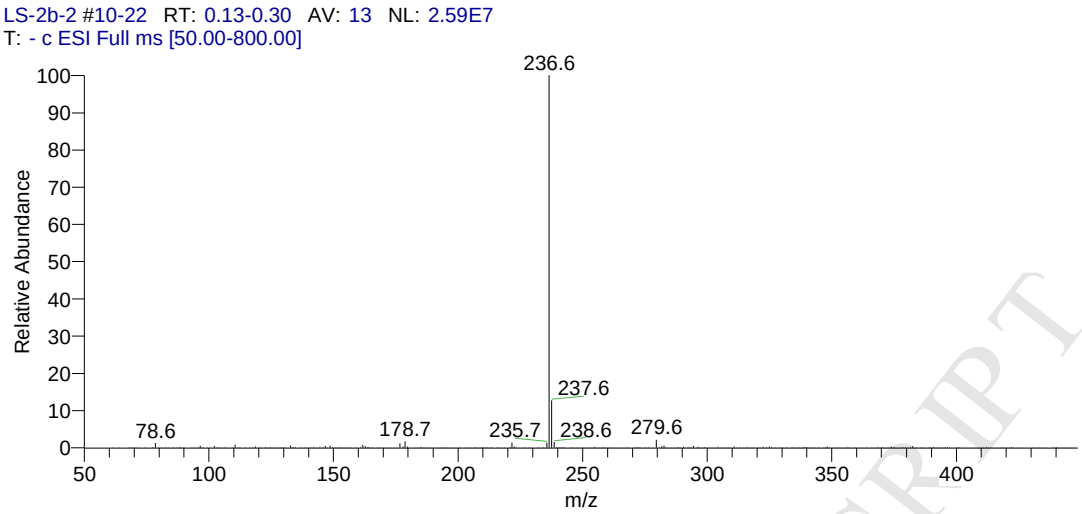

Figure 3. MS spectrum of 2b

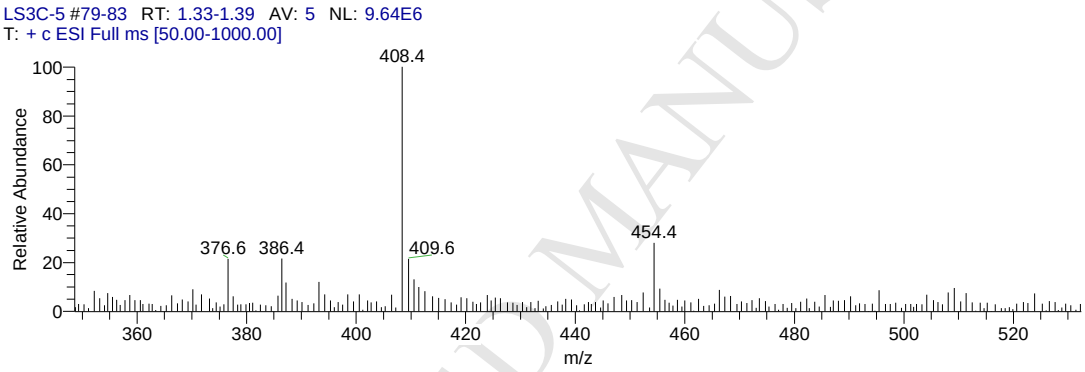

Figure 4. MS spectrum of 2c

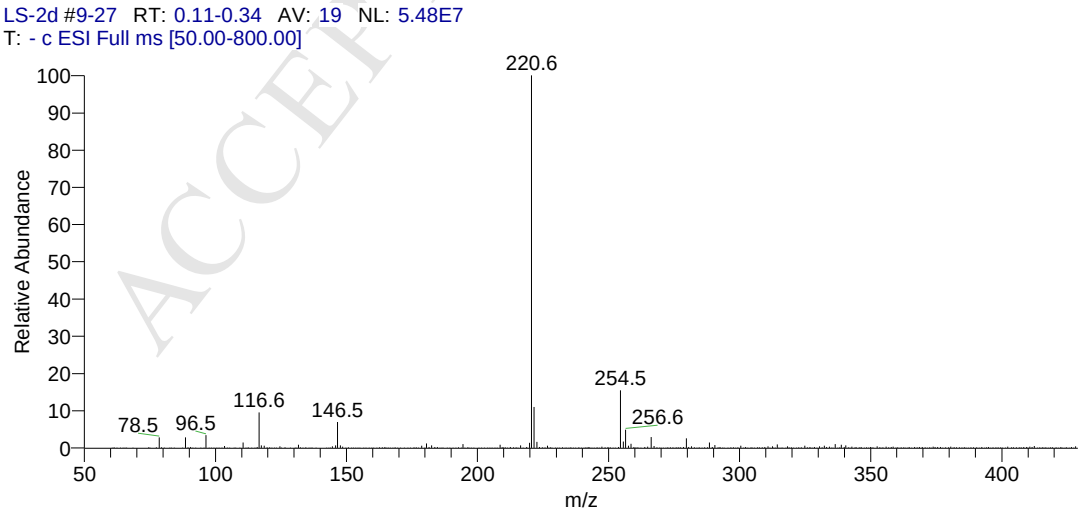

Figure 5. MS spectrum of 2d

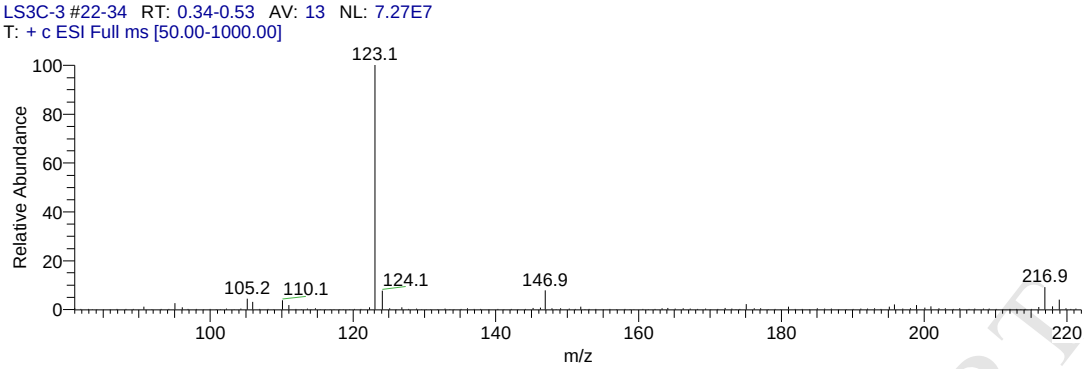

Figure 6. MS spectrum of oxime 1

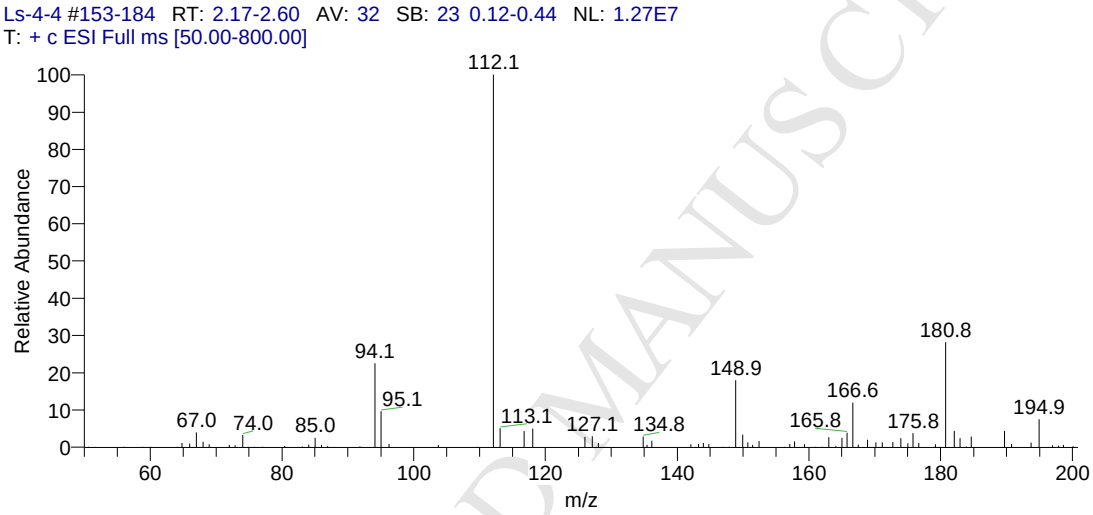

Figure 7. MS spectrum of oxime 2

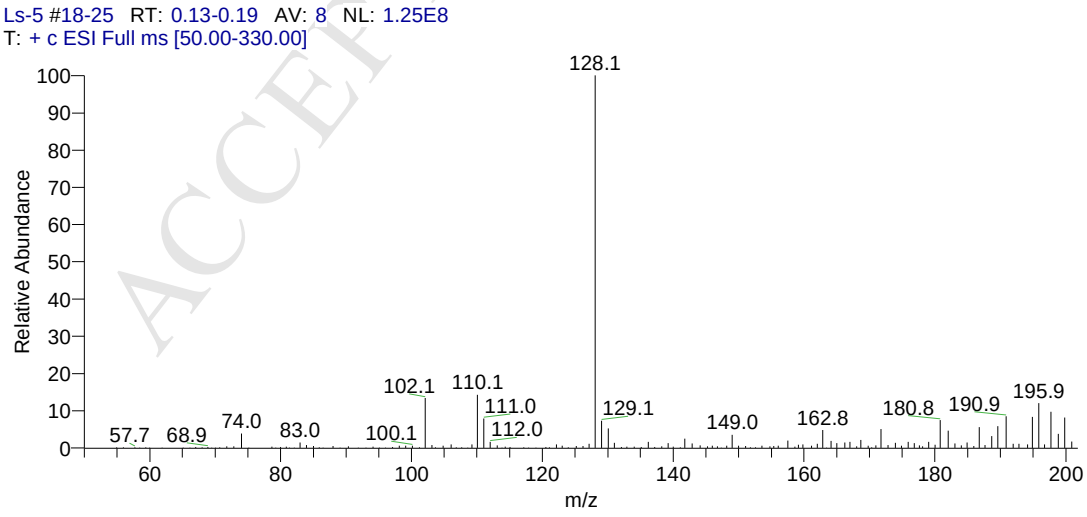

Figure 8. MS spectrum of oxime 3

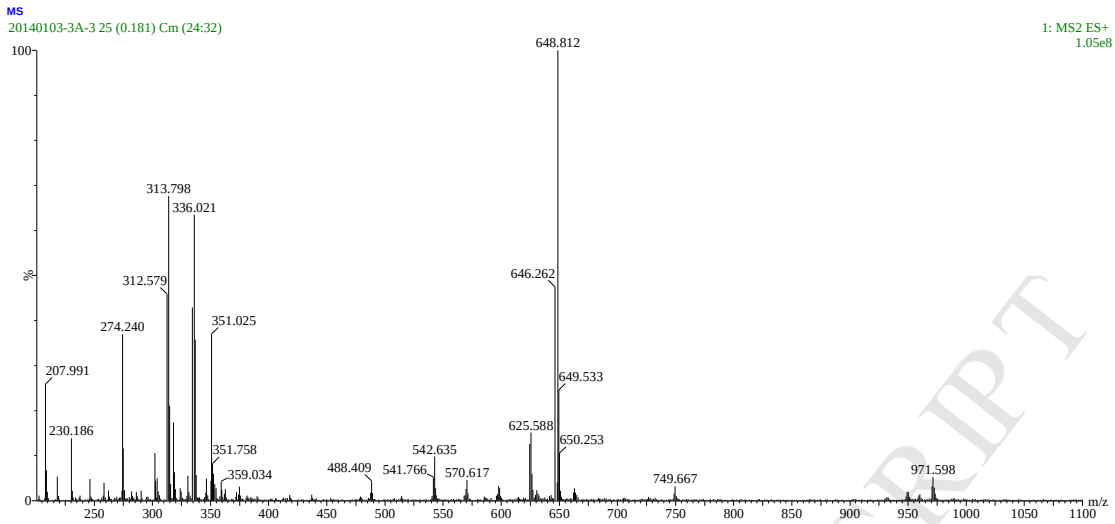

99

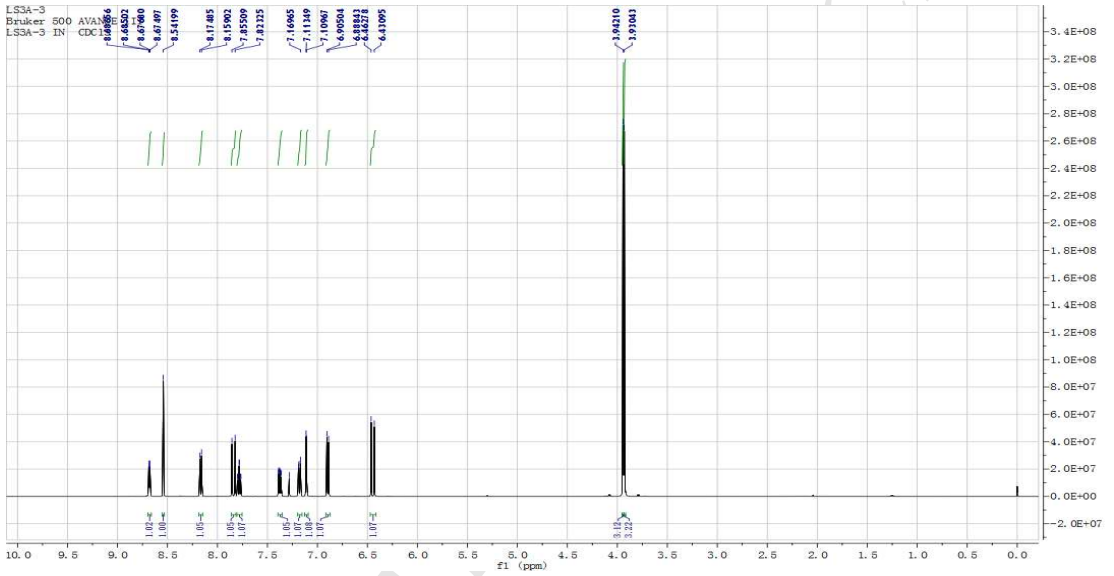

100

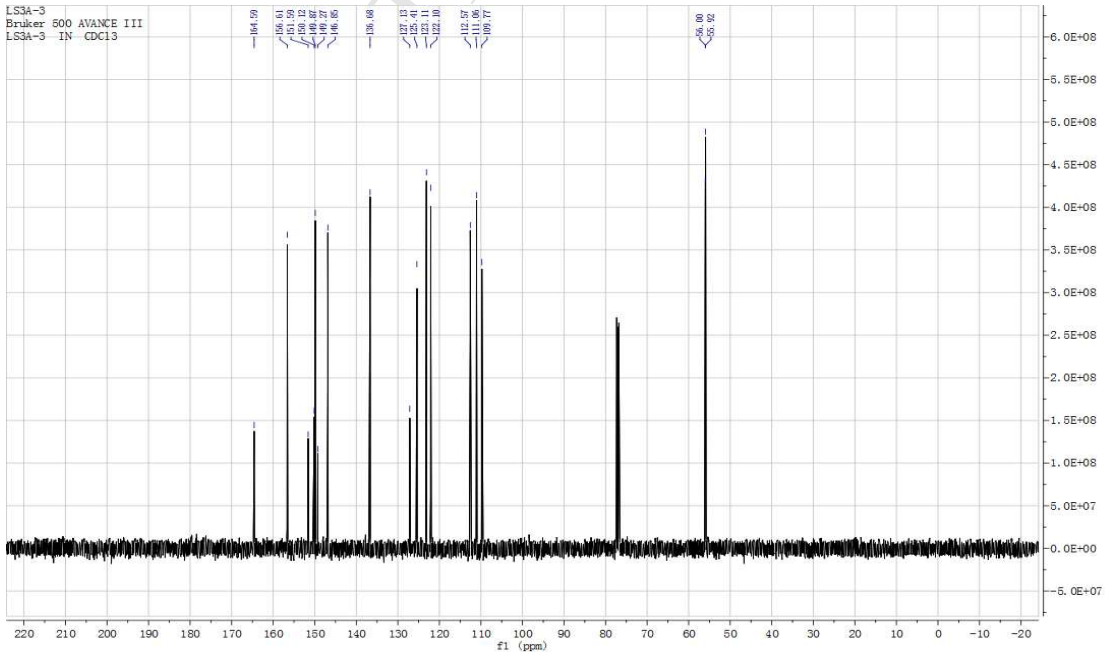

101

102 Figure 9. MS, ^{1}H NMR and ^{13}C NMR spectrum of 4a-1

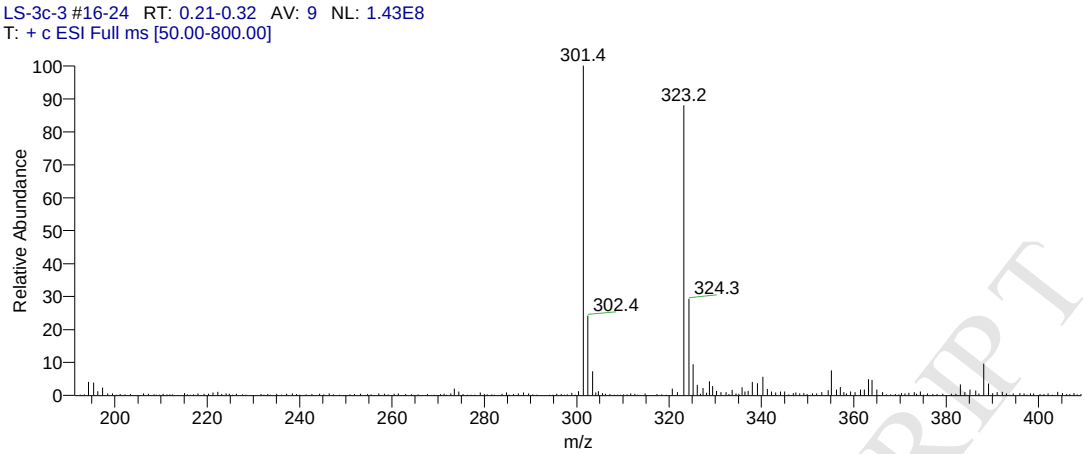

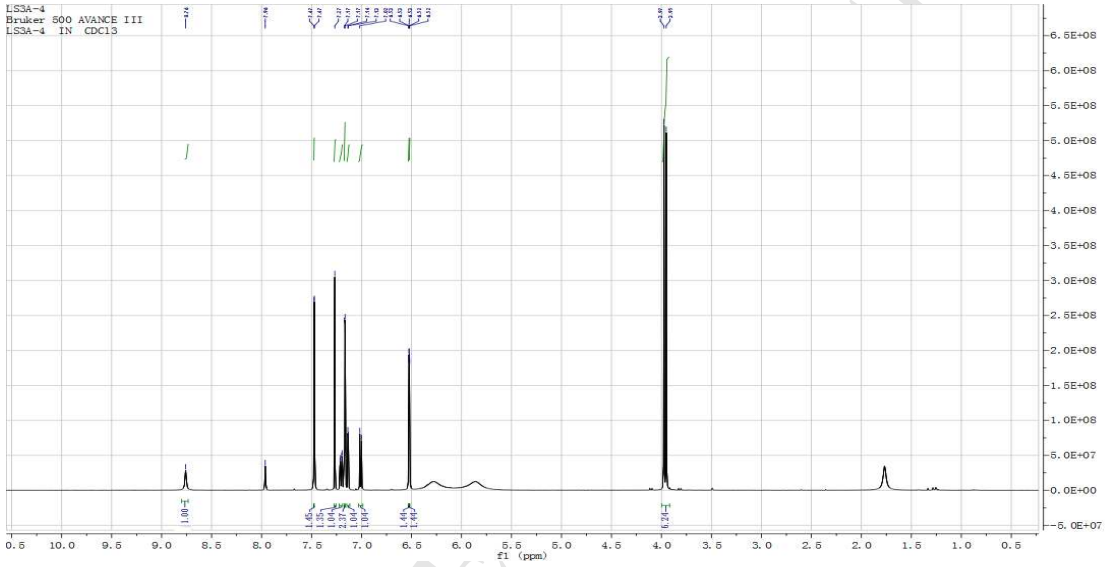

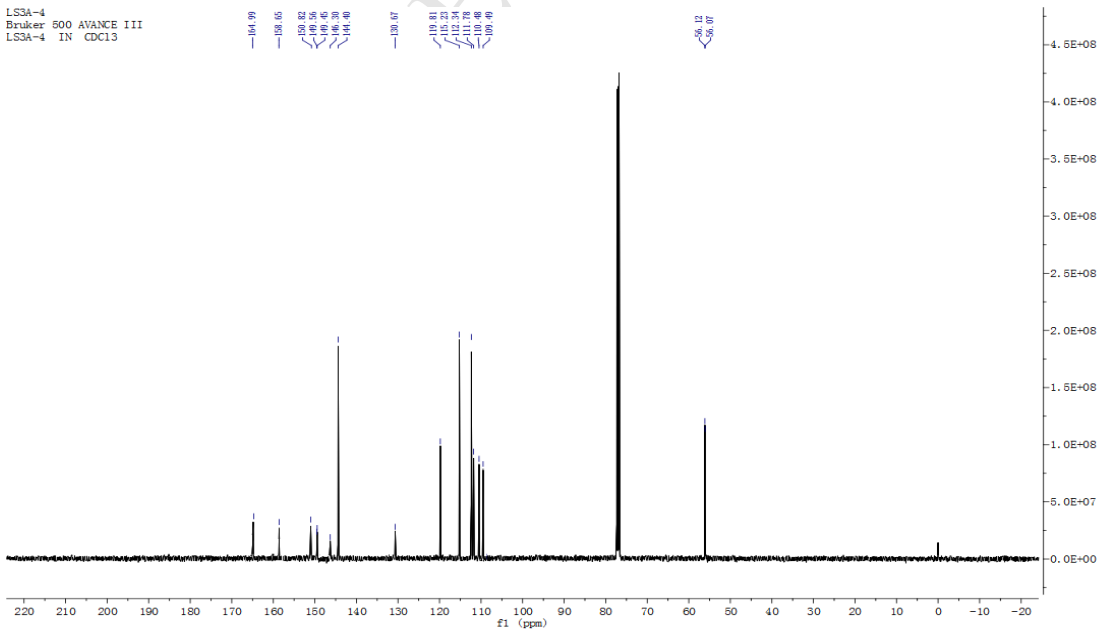

Figure 10. MS, ^{1}H NMR and ^{13}C NMR spectrum of 4a-2

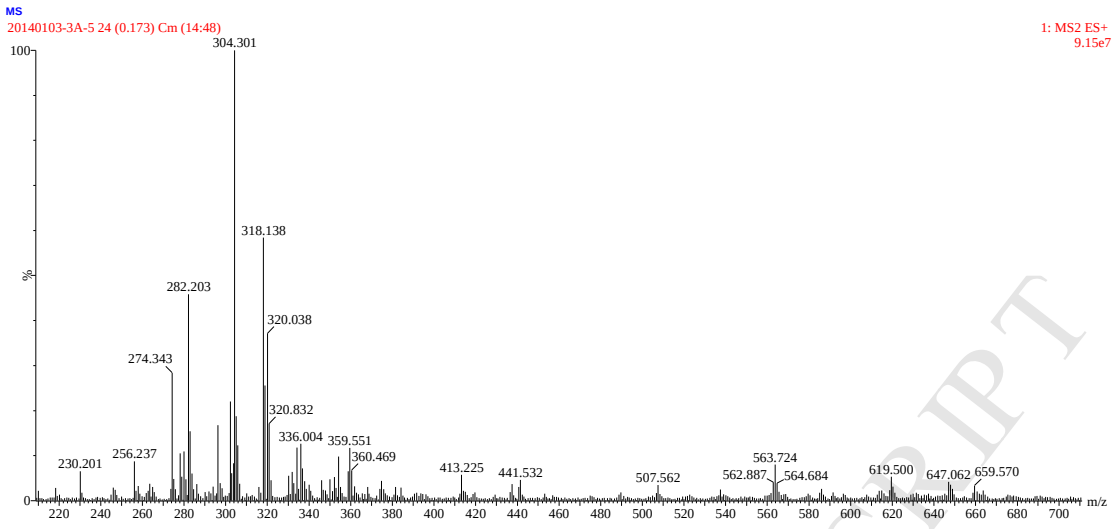

109

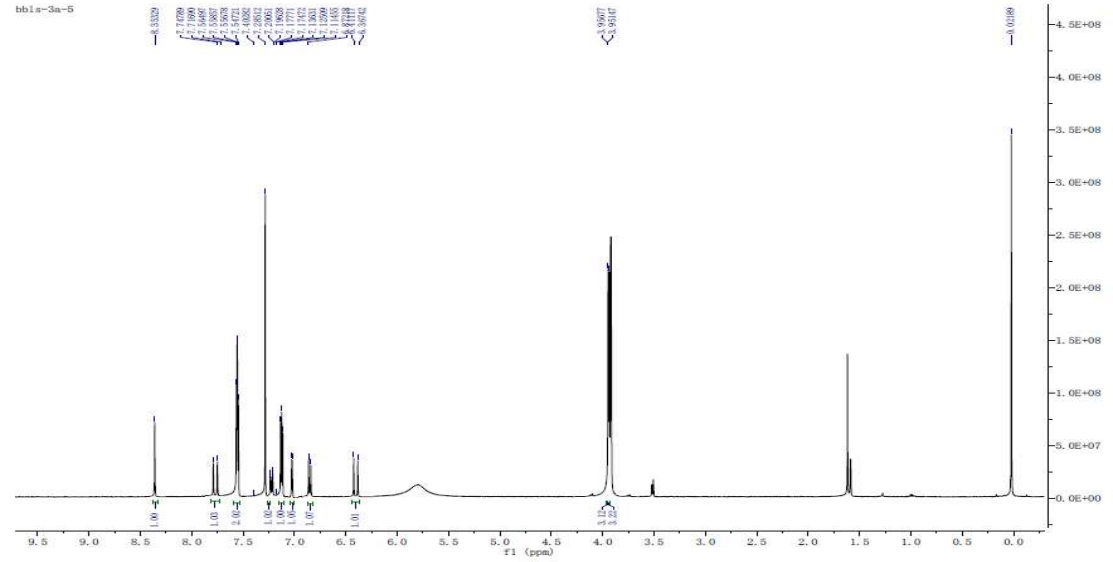

110

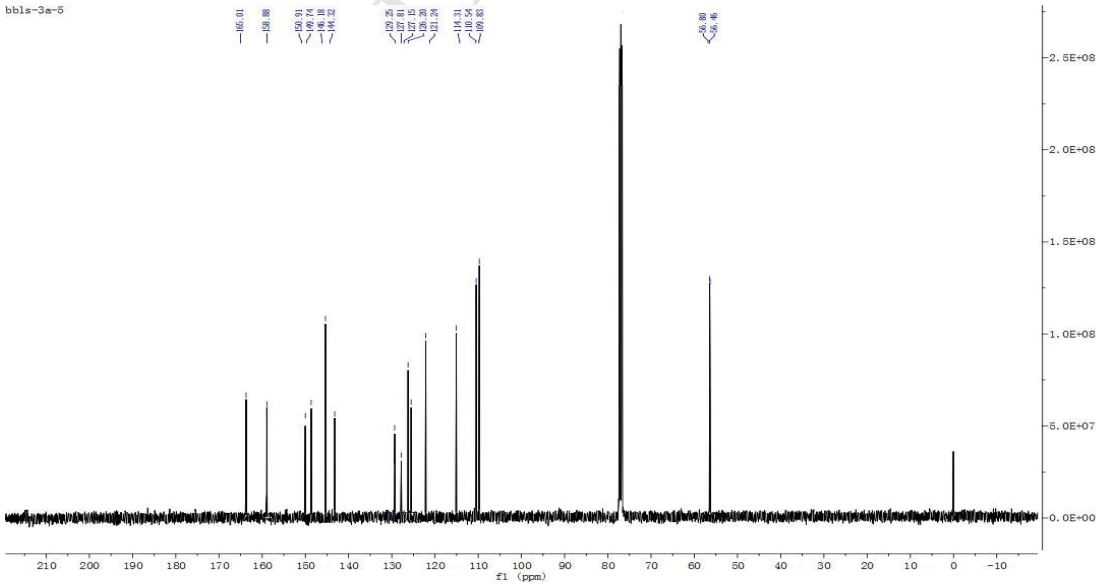

111

112 Figure 11. MS, ^{1}H NMR and ^{13}C NMR spectrum of 4a-3

113

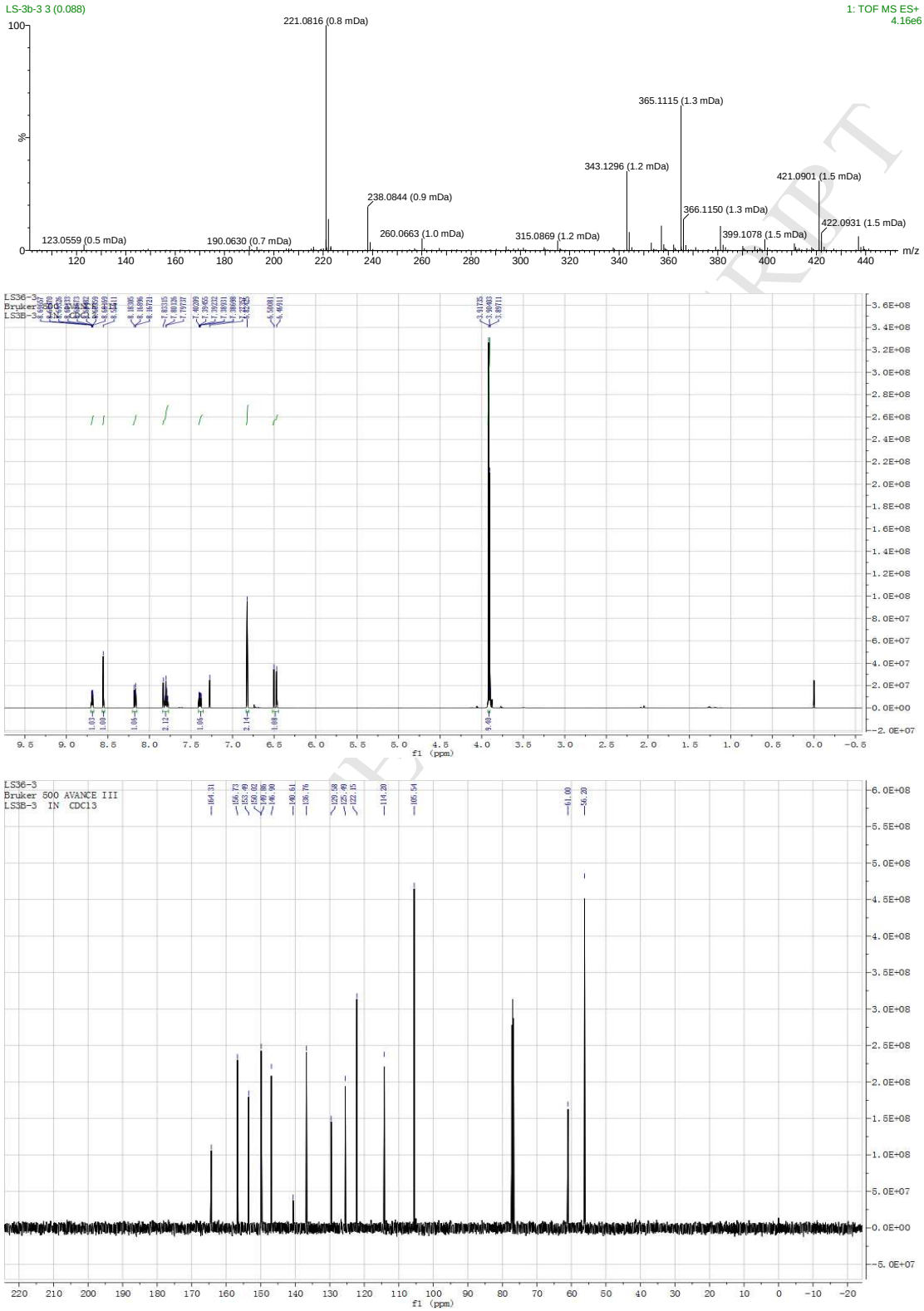

Figure 12. MS, ^{1}H NMR and ^{13}C NMR spectrum of 4b-1

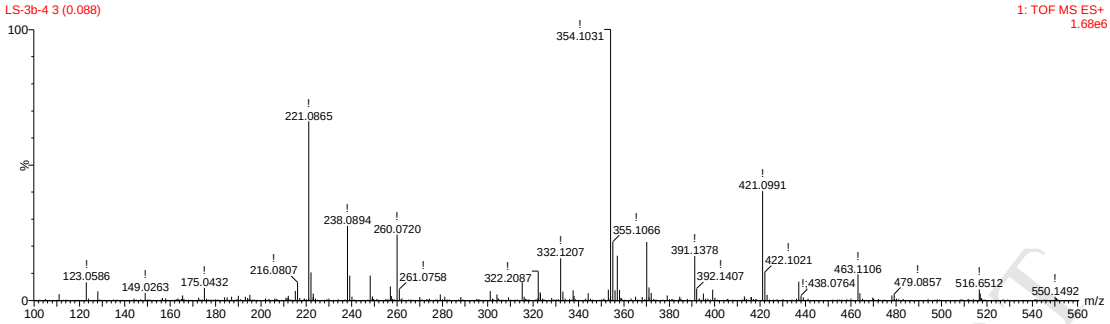

121

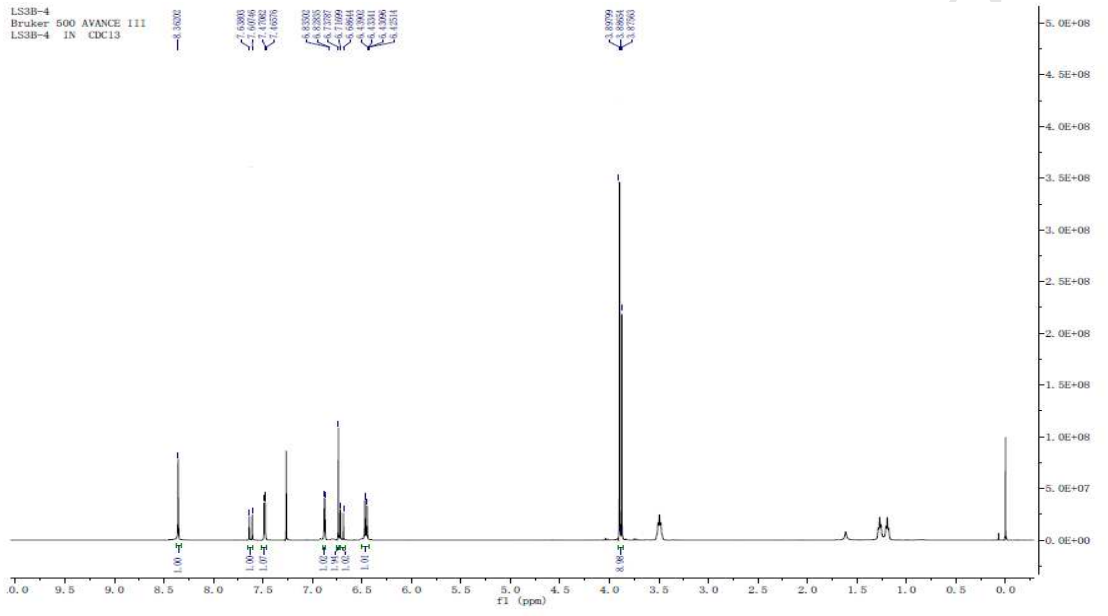

122

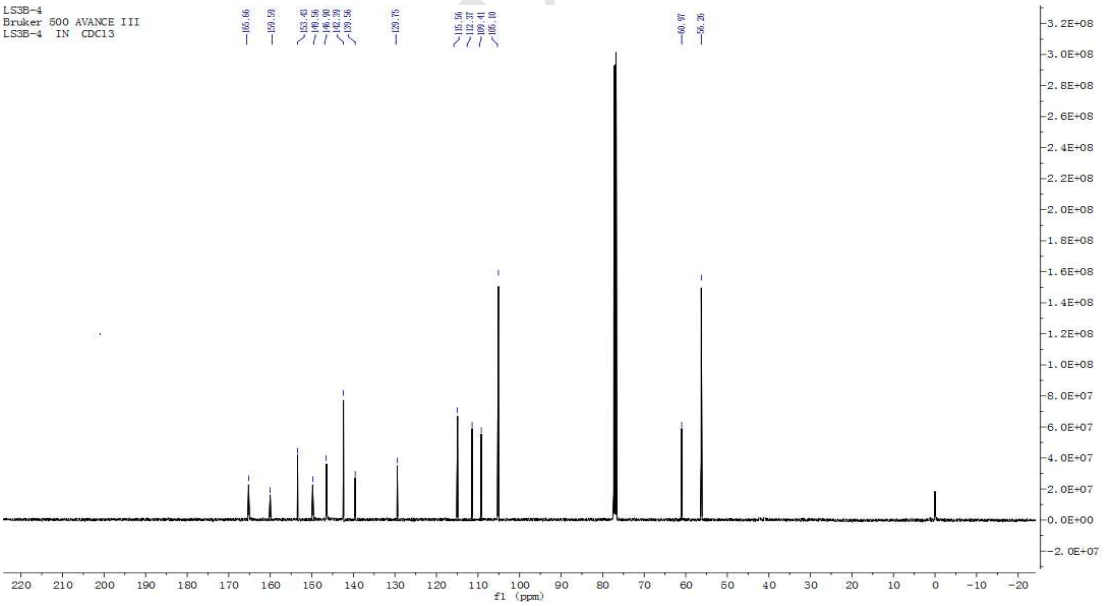

123

124 Figure 13. MS, ^{1}H NMR and ^{13}C NMR spectrum of 4b-2

125

126

127

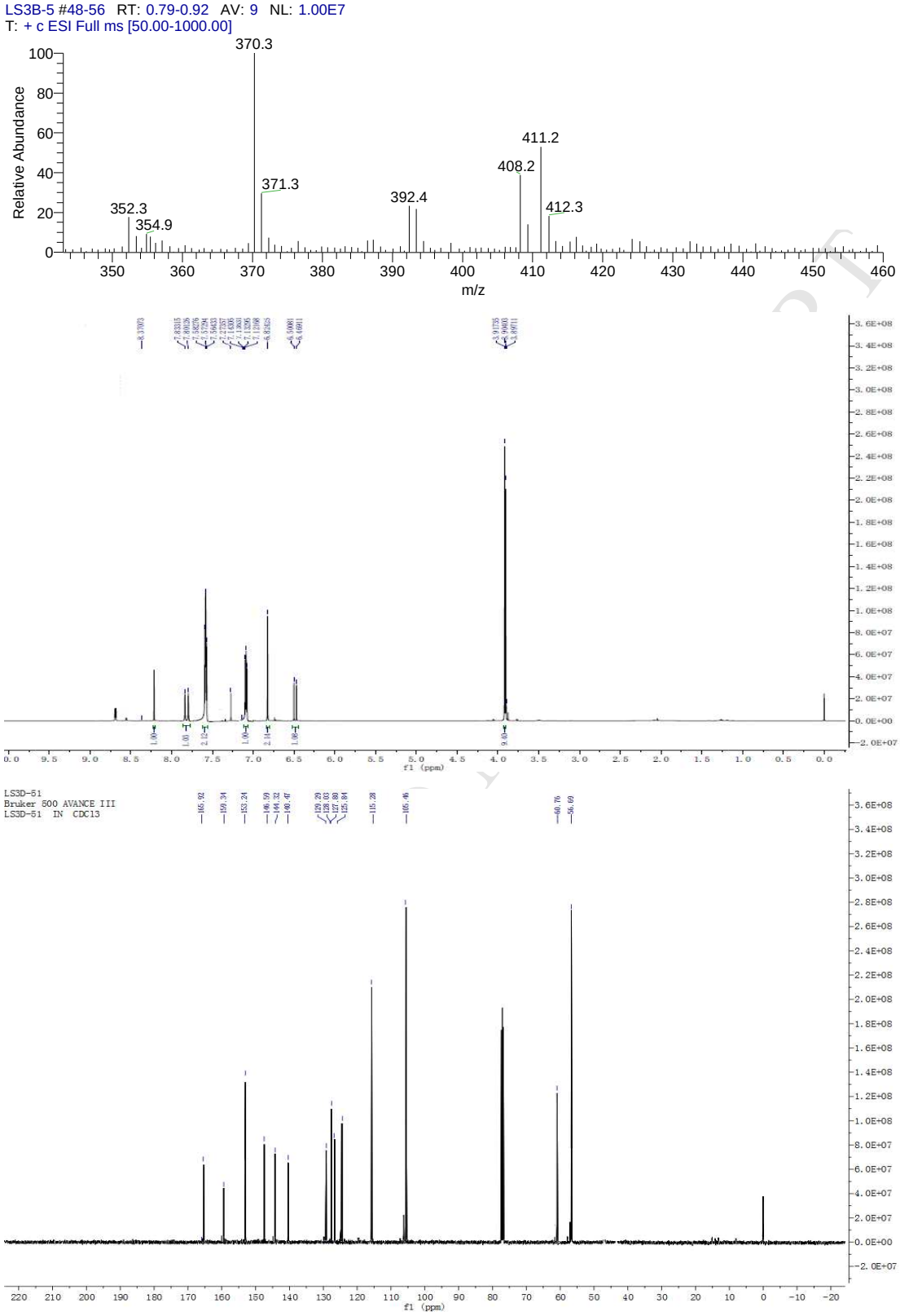

Figure 14. MS, ^{1}H NMR and ^{13}C NMR spectrum of 4b-3

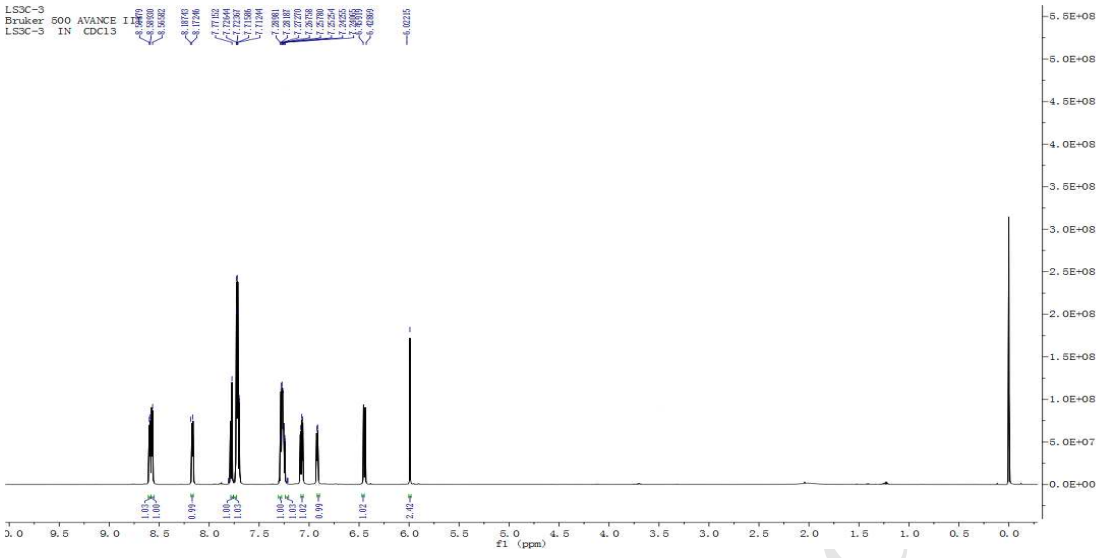

135

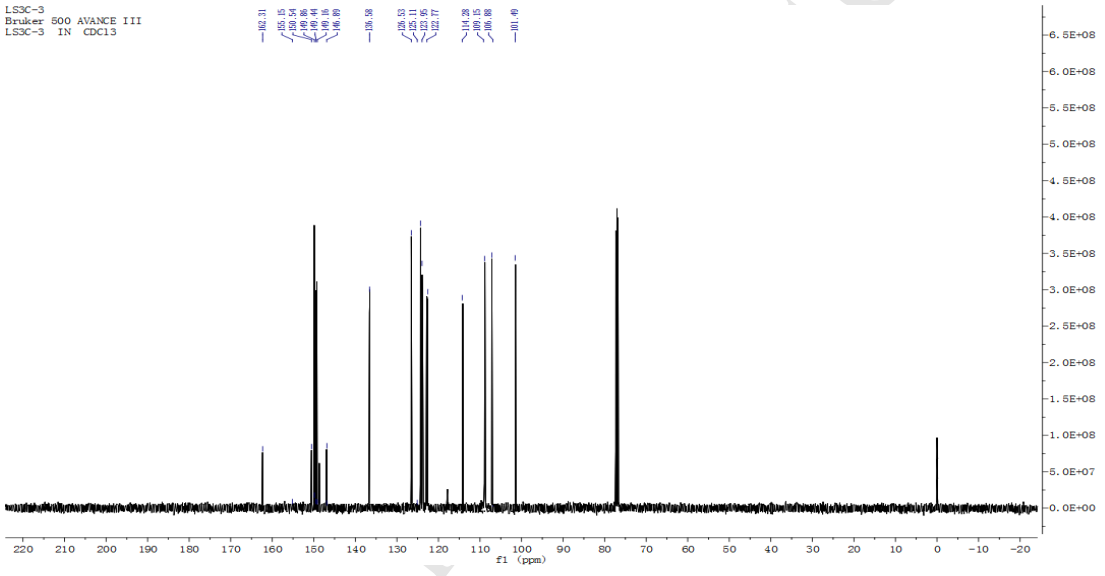

136

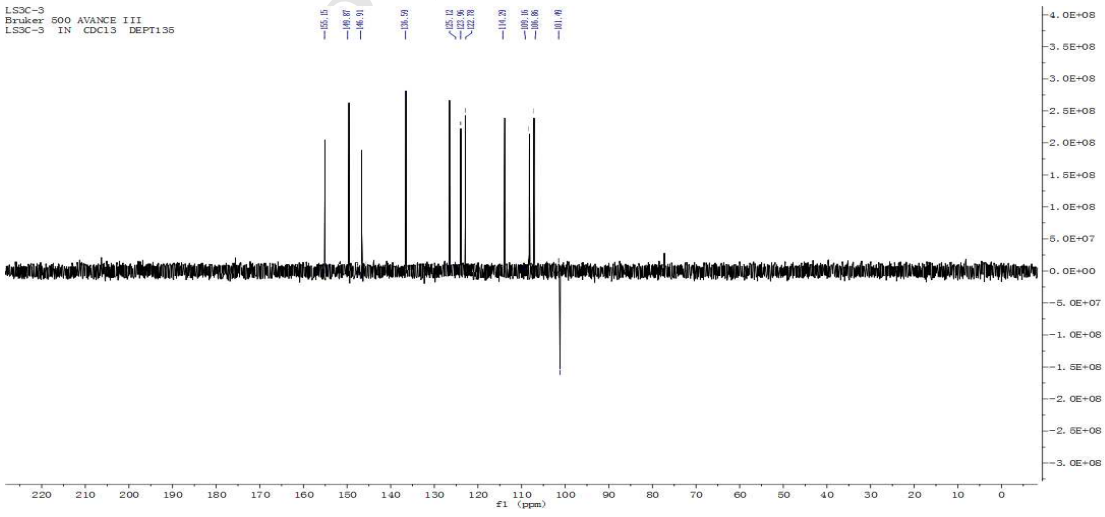

137

138 Figure 15. MS, ^{1}H NMR and ^{13}C NMR spectrum of 4c-1

139

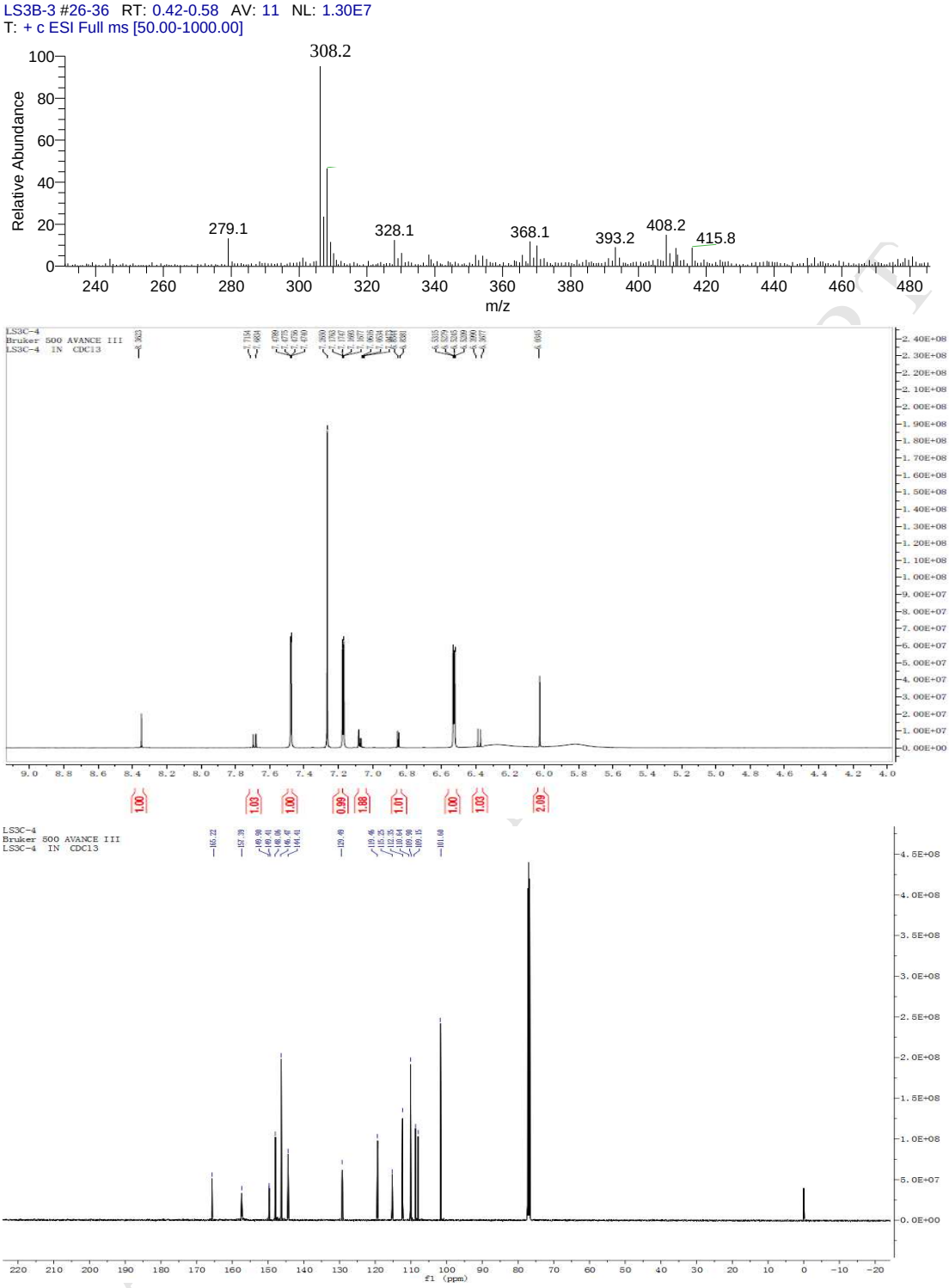

Figure 16. MS, ^{1}H NMR and ^{13}C NMR spectrum of 4c-2

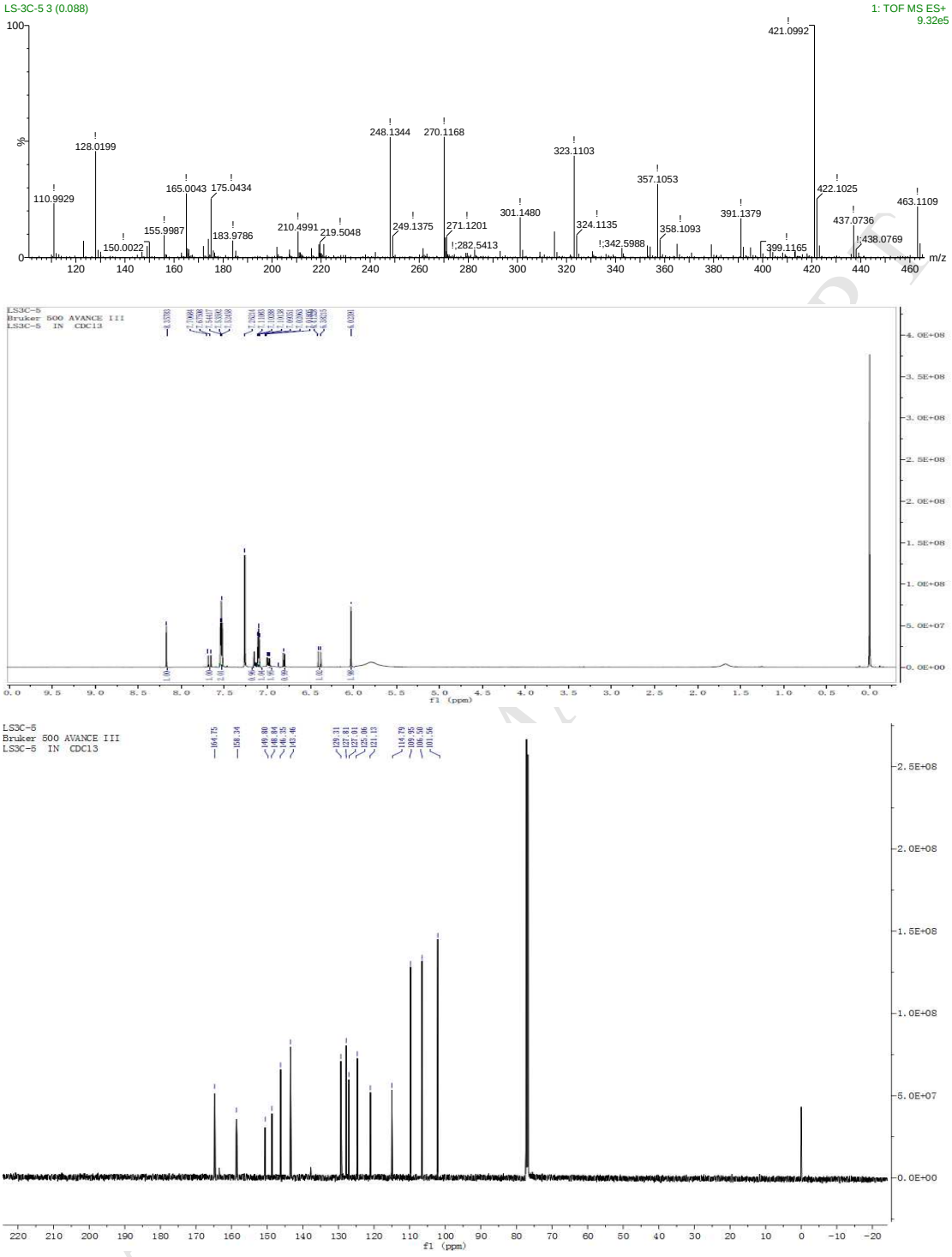

Figure 17. MS, ^{1}H NMR and ^{13}C NMR spectrum of 4c-3

158

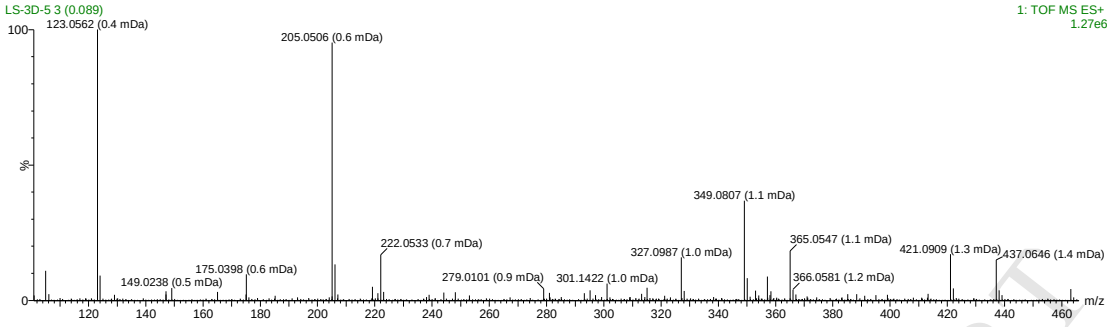

159

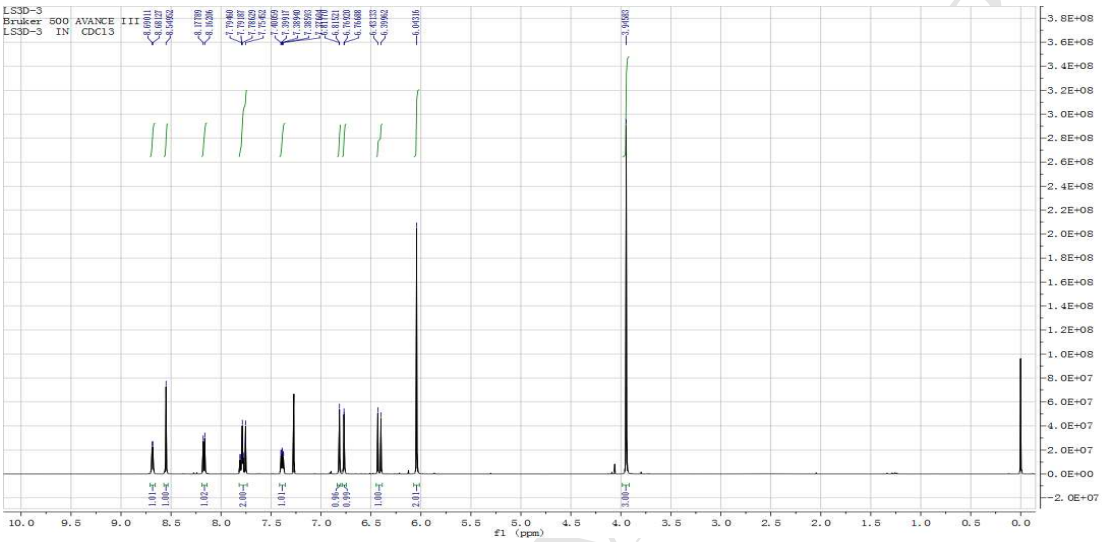

160

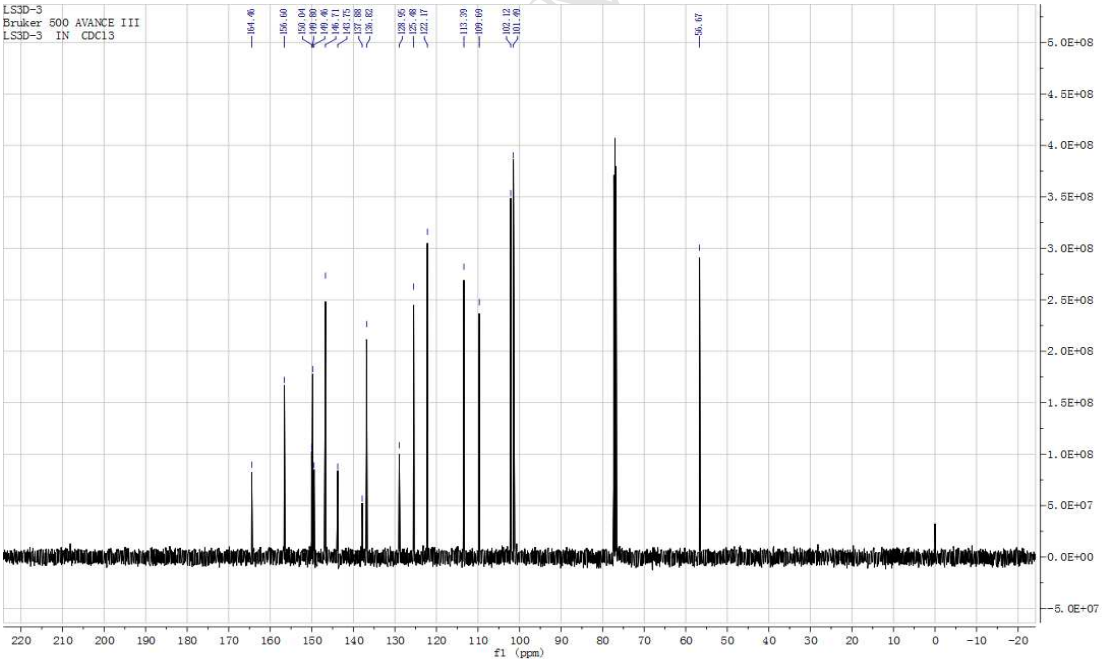

161 Figure 18. MS, ^{1}H NMR and ^{13}C NMR spectrum of 4d-1

162

163

164

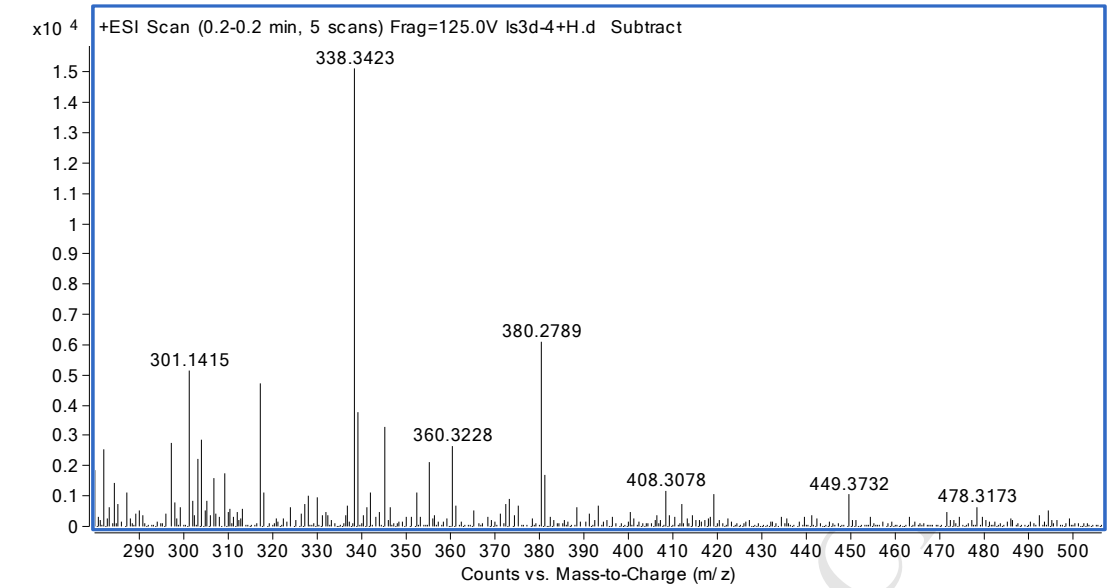

165

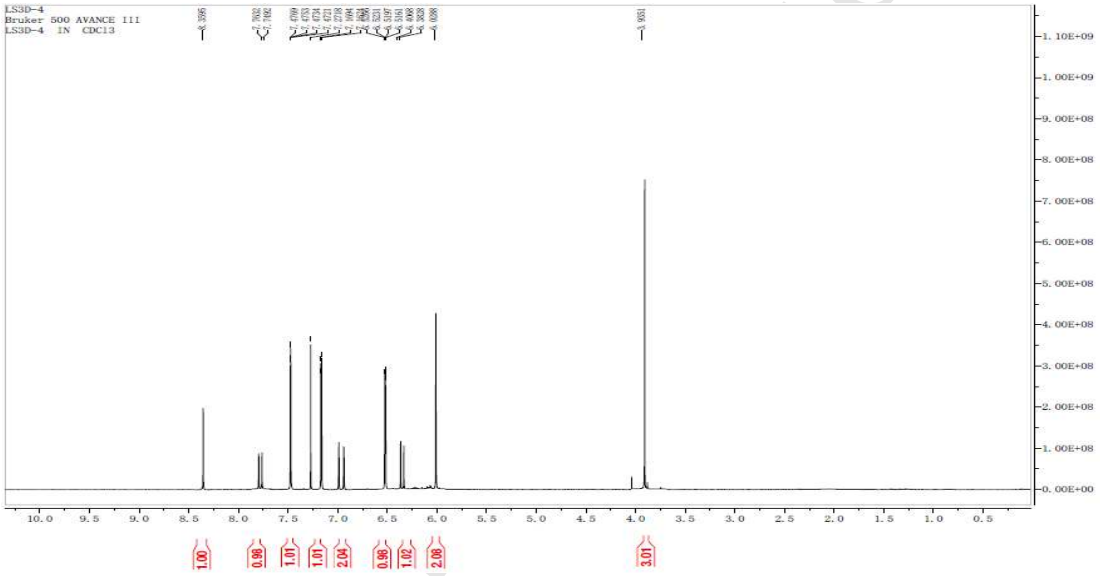

166

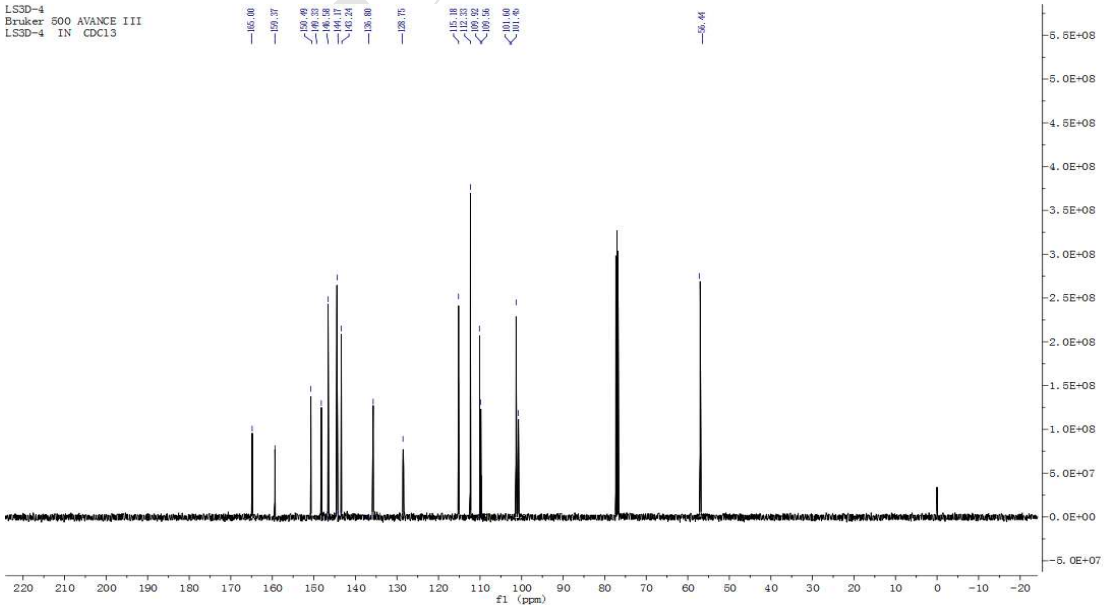

167

168 Figure 19. MS, ^{1}H NMR and ^{13}C NMR spectrum of 4d-2

169

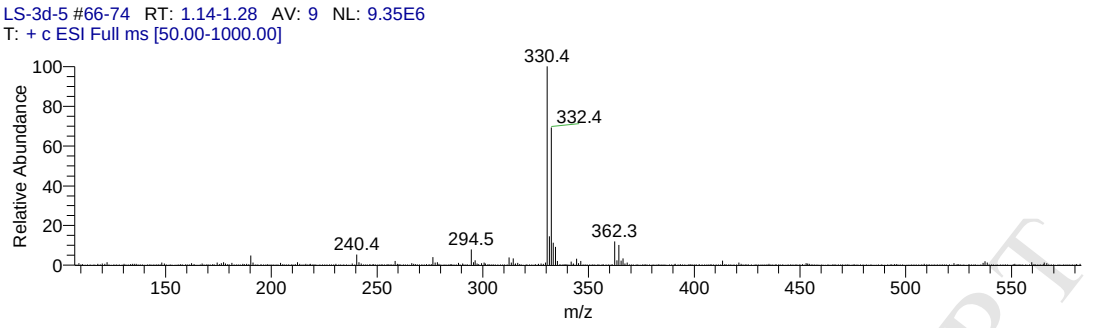

170

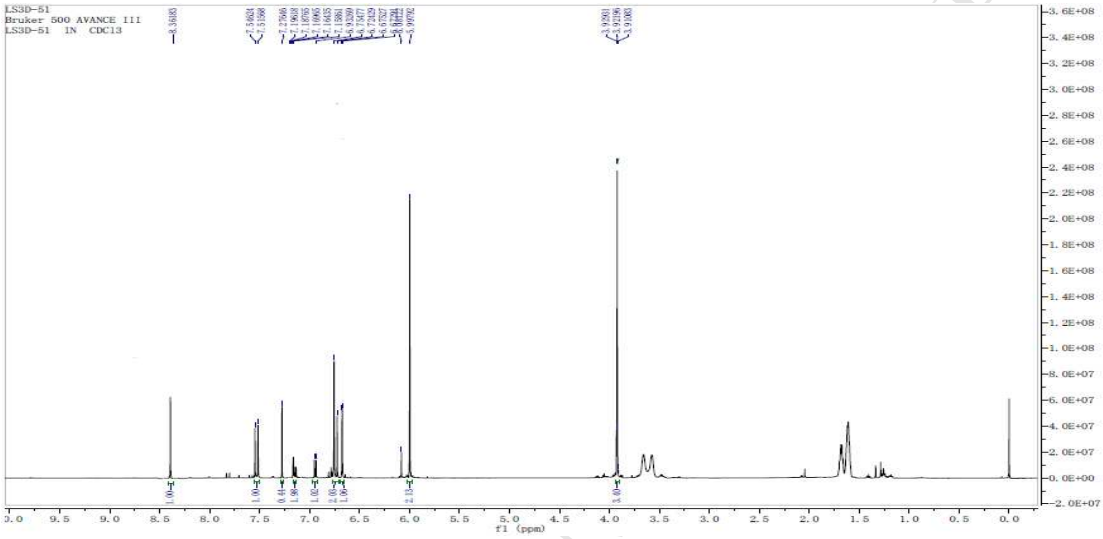

171

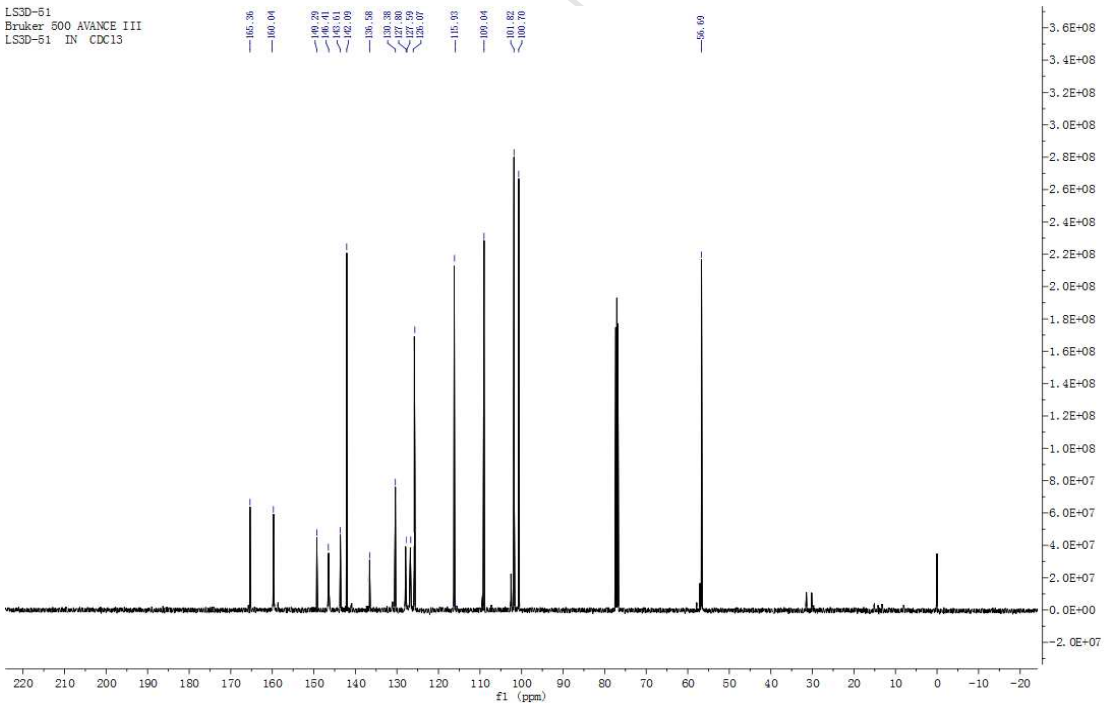

172

173 Figure 20. MS, ^{1}H NMR and ^{13}C NMR spectrum of 4d-3

174

175

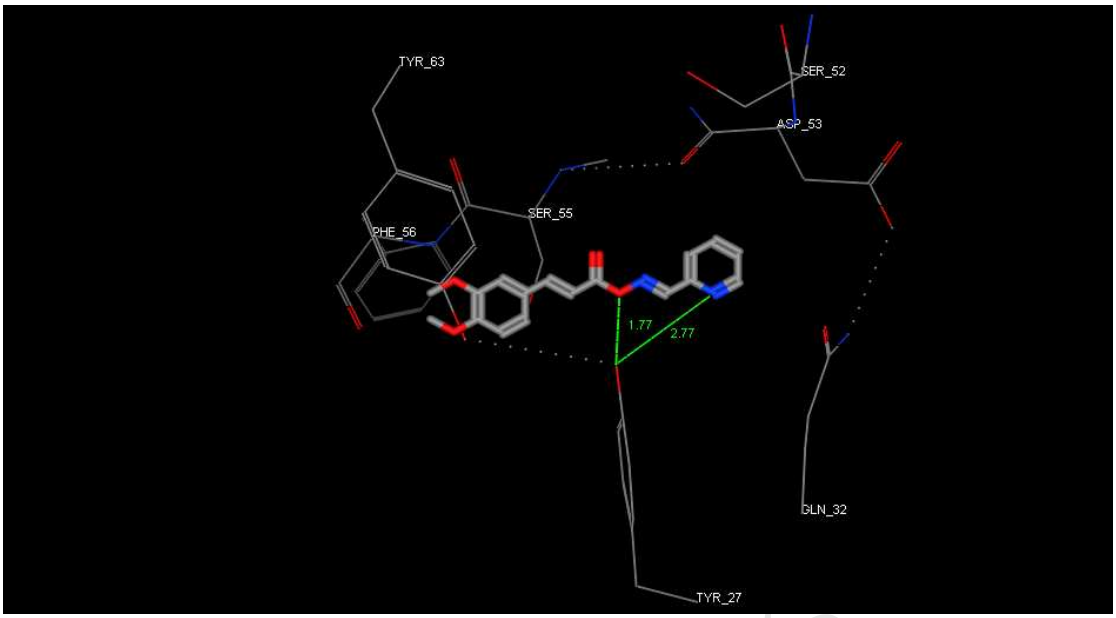

Figure 21. Binding mode of compound 4a-1 into the binding site of HLA-A.

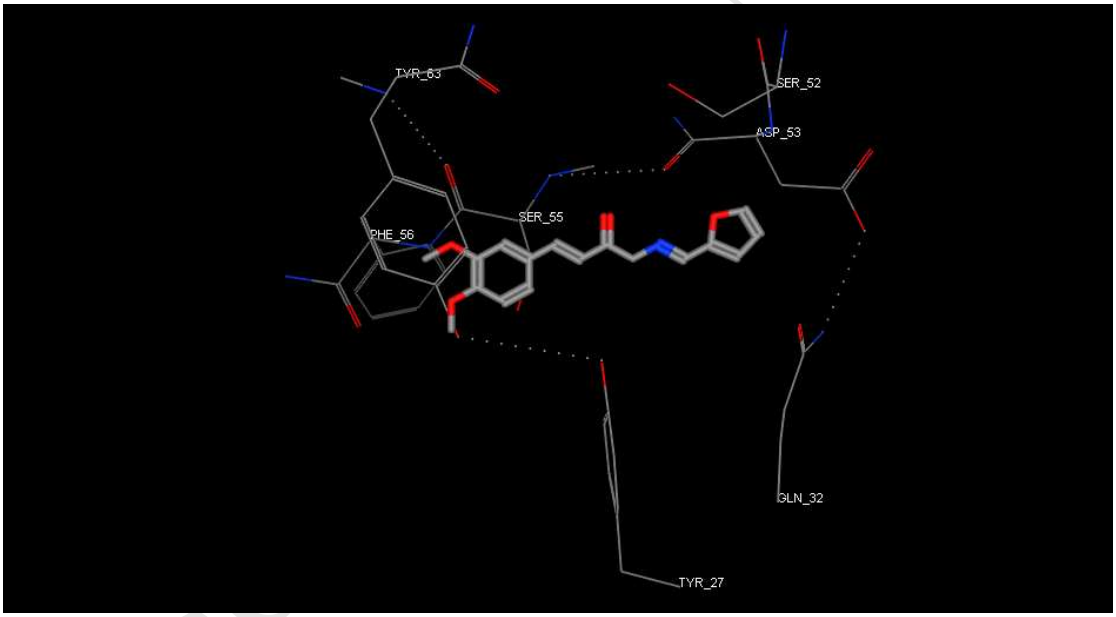

Figure 22. Binding mode of compound 4a-2 into the binding site of HLA-A.

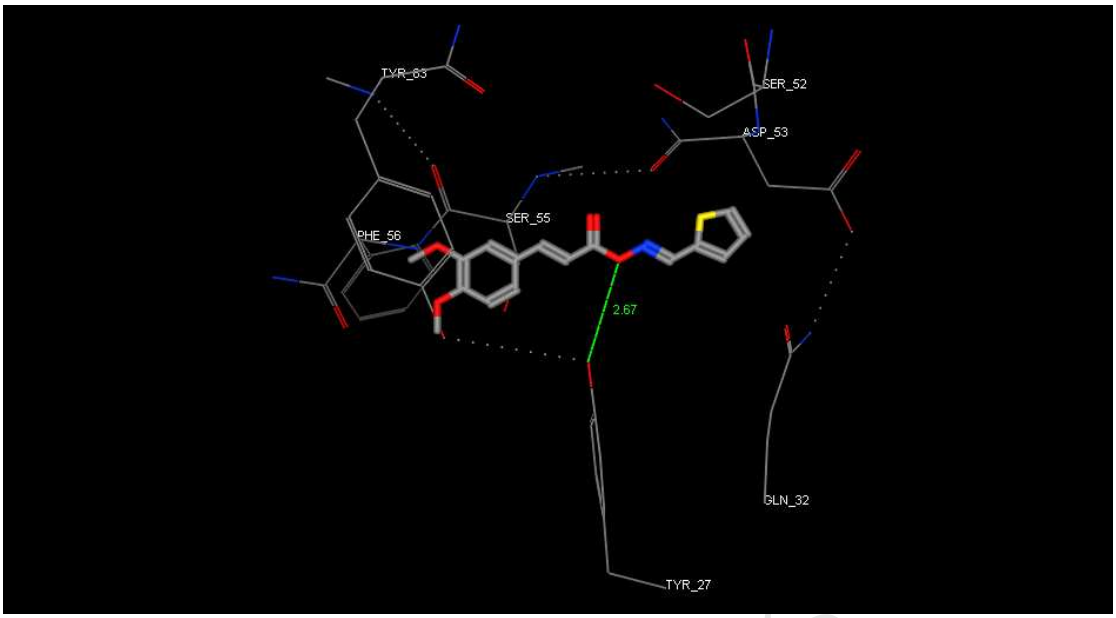

Figure 23. Binding mode of compound 4a-3 into the binding site of HLA-A.

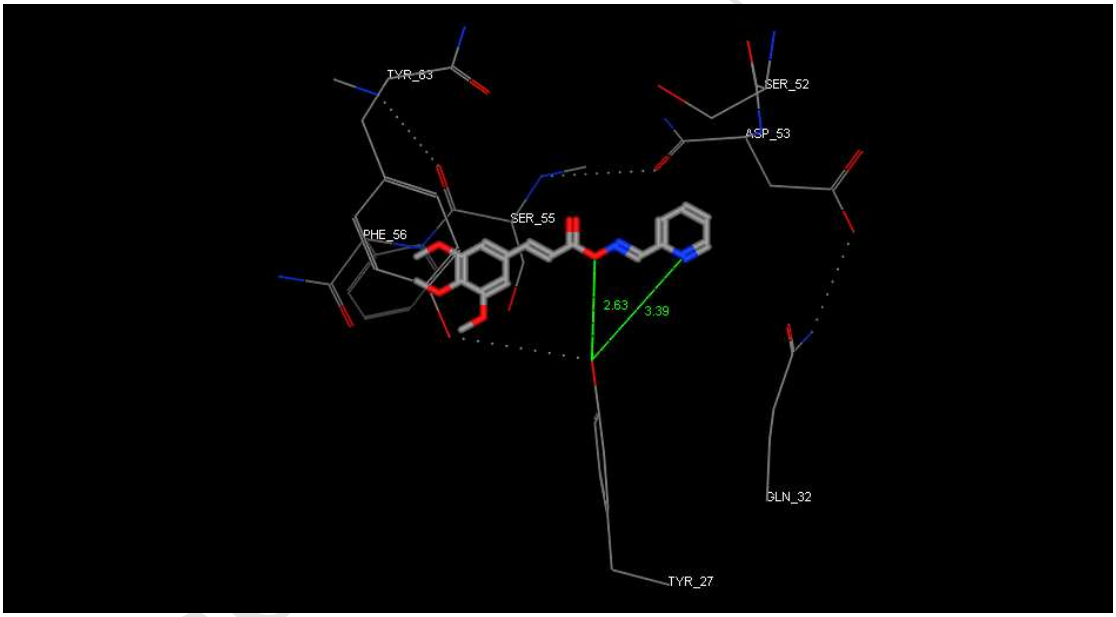

Figure 24. Binding mode of compound 4b-1 into the binding site of HLA-A.

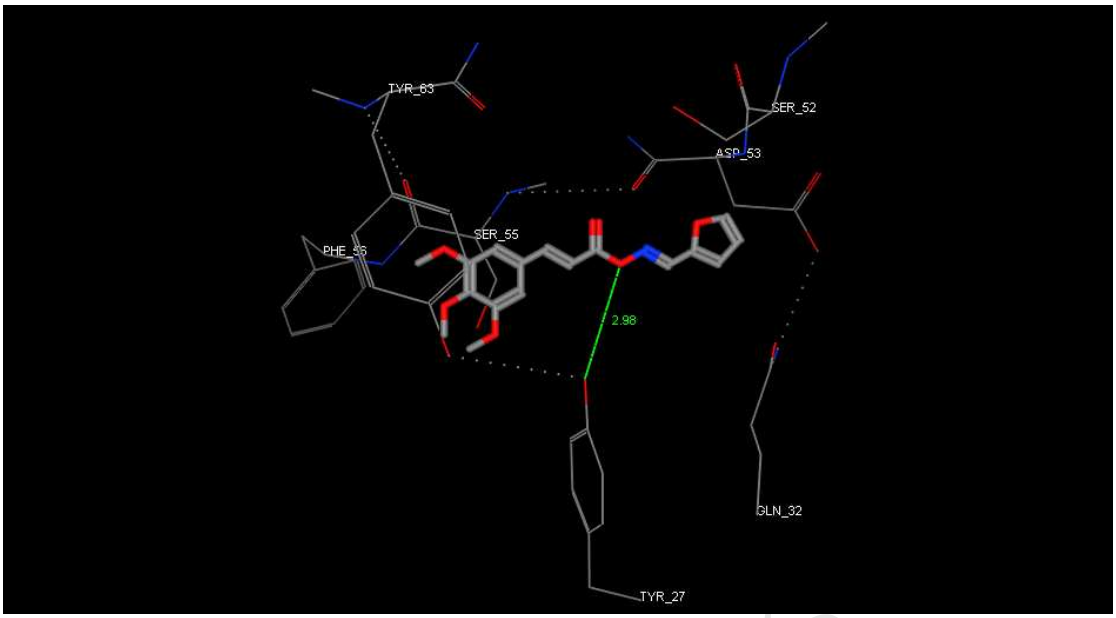

Figure 25. Binding mode of compound 4b-2 into the binding site of HLA-A.

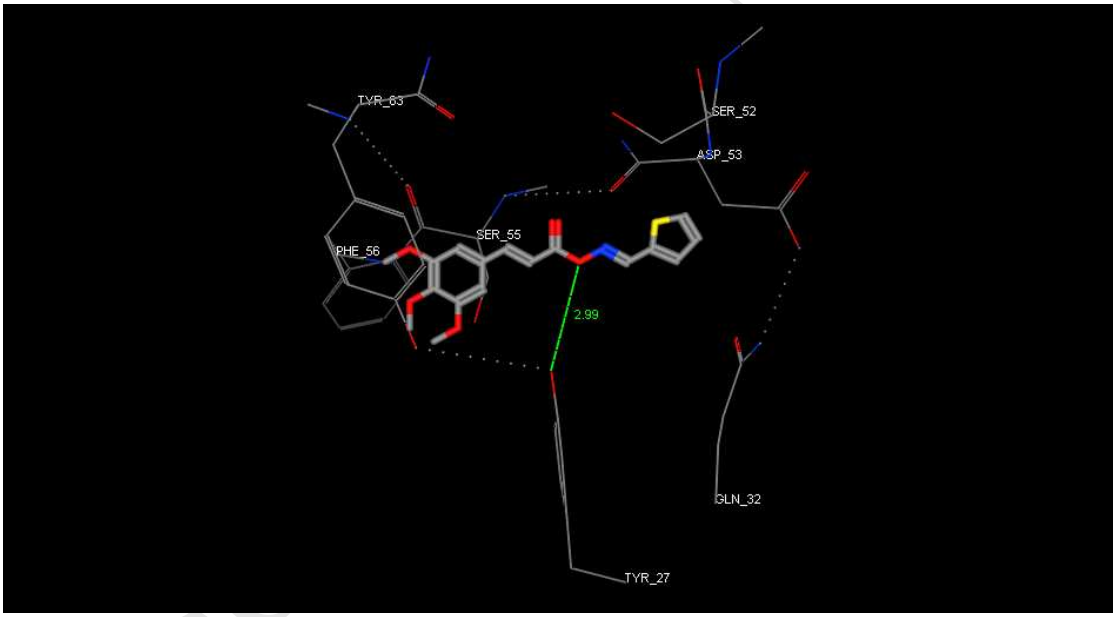

Figure 26. Binding mode of compound 4b-3 into the binding site of HLA-A.

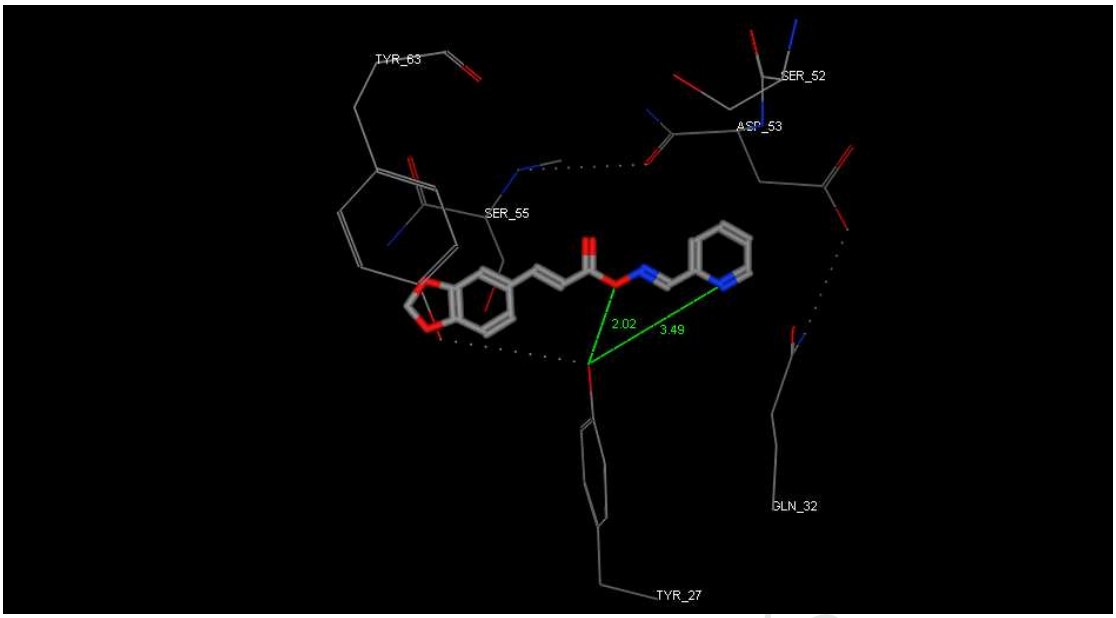

Figure 27. Binding mode of compound 4c-1 into the binding site of HLA-A.

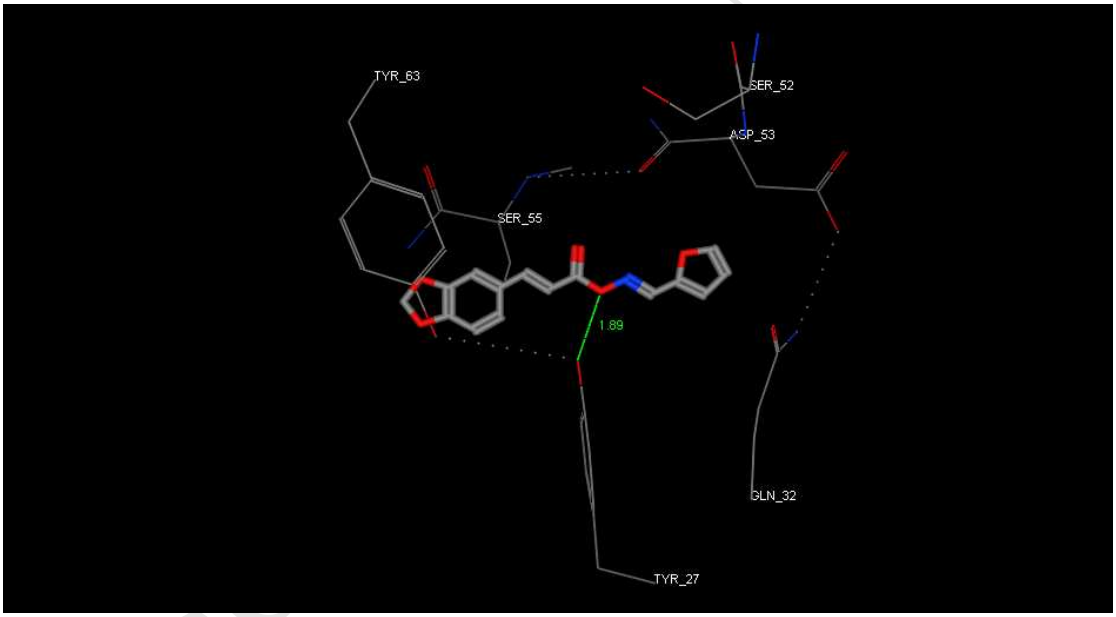

Figure 28. Binding mode of compound 4c-2 into the binding site of HLA-A.

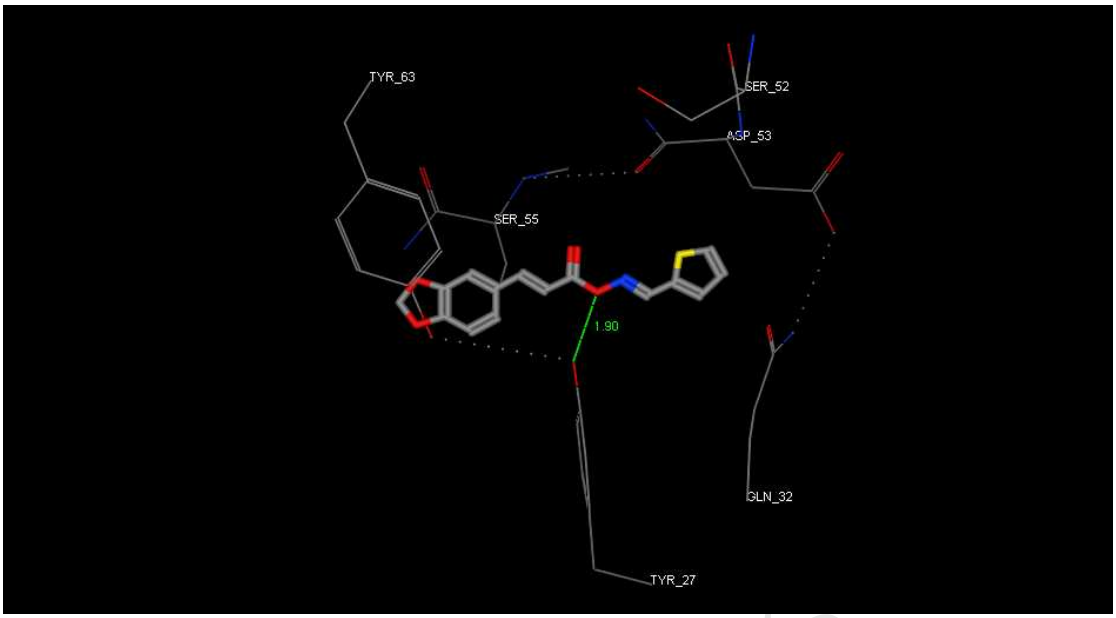

Figure 29. Binding mode of compound 4c-3 into the binding site of HLA-A.

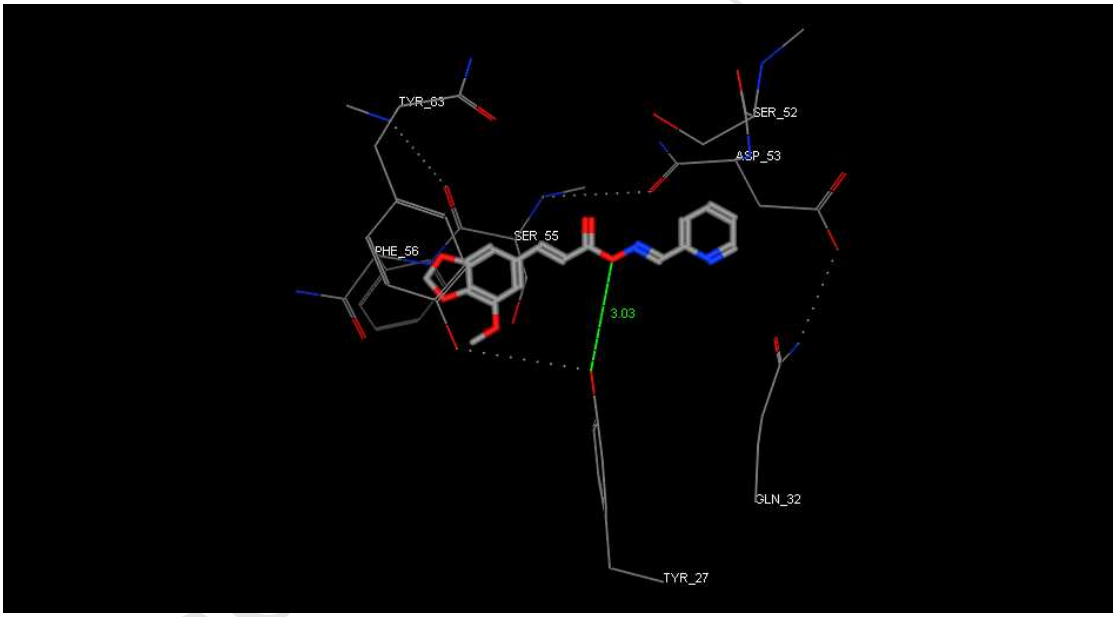

Figure 30. Binding mode of compound 4d-1 into the binding site of HLA-A.

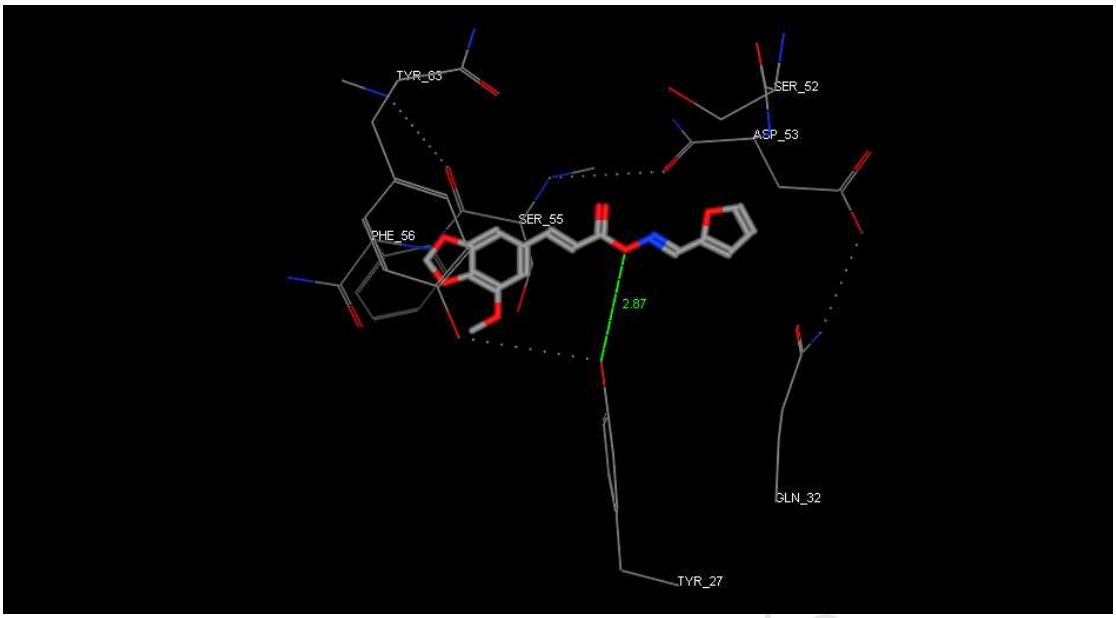

Figure 31. Binding mode of compound 4d-2 into the binding site of HLA-A.

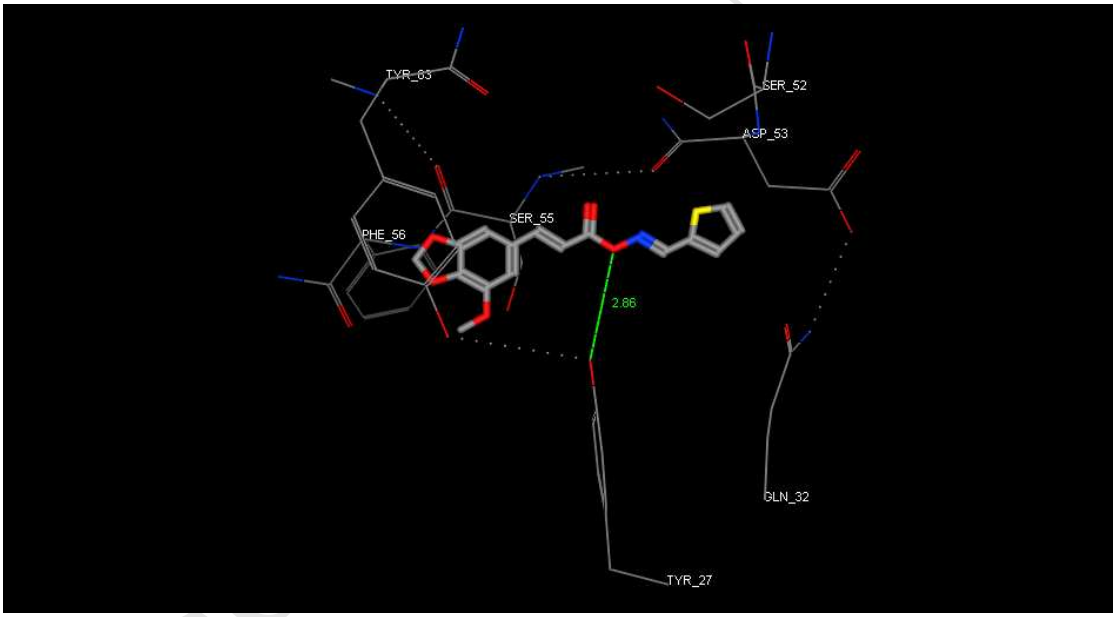

Figure 32. Binding mode of compound 4d-3 into the binding site of HLA-A.

220 Table 1. Effects of on the inhibition of HBsAg secretion by HepG2.2.15 cells ($\bar{x}$±s, n=3).

Groups	Concentration/ μM	3 days		6 days		9 days		9 days
		OD ($\bar{x}$±s)	Inhibition (%)	OD ($\bar{x}$±s)	Inhibition (%)	OD ($\bar{x}$±s)	Inhibition (%)	Cell survival (%)
Control	-	0.632±0.052	-	0.548±0.026	-	0.218±0.015	-	100
3TC	300	0.426±0.038	37.26	0.344±0.027	43.59	0.129±0.025	60.36	75.19
	150	0.474±0.026	28.56	0.404±0.028	30.70	0.135±0.038	55.86	82.39
	75	0.511±0.046	21.98	0.435±0.043	24.15	0.169±0.031	33.11	95.86
	37.5	0.568±0.033	11.59	0.511±0.030	7.98	0.181±0.041	25.23	118.45
4a-1	300	0.558±0.051	13.35	0.394±0.037	32.83	0.127±0.018	61.26	99.54
	150	0.573±0.044	10.75	0.423±0.025	26.78	0.137±0.022	54.50	101.86
	75	0.618±0.044	2.54	0.457±0.040	19.52	0.164±0.008	36.71	104.25
	37.5	0.647±0.026	-	0.495±0.016	11.25	0.189±0.013	19.82	106.67
4a-2	300	0.371±0.017	47.22	0.296±0.039	53.77	0.137±0.015	54.95	103.31
	150	0.413±0.026	39.67	0.341±0.026	44.23	0.148±0.017	47.30	114.02
	75	0.446±0.035	33.64	0.377±0.022	36.54	0.160±0.012	39.41	120.16
	37.5	0.522±0.034	19.87	0.451±0.019	20.80	0.187±0.031	21.17	128.25
4a-3	300	0.369±0.047	47.64	0.247±0.034	52.64	0.136±0.013	54.95	97.71
	150	0.407±0.038	40.70	0.285±0.032	41.24	0.155±0.033	42.79	98.65
	75	0.475±0.036	28.44	0.366±0.037	29.56	0.175±0.065	29.28	101.20
	37.5	0.536±0.054	17.39	0.432±0.032	19.80	0.187±0.024	20.50	113.67
4b-1	300	0.549±0.036	15.10	0.359±0.020	40.46	0.166±0.027	66.67	88.95
	150	0.586±0.023	8.39	0.409±0.016	29.63	0.188±0.020	47.30	98.07
	75	0.616±0.051	2.96	0.467±0.030	17.24	0.200±0.016	39.19	106.92
	37.5	0.641±0.028	-	0.489±0.063	12.68	0.216±0.031	24.10	108.25
4b-2	300	0.429±0.031	36.71	0.313±0.031	50.14	0.128±0.017	60.81	76.08
	150	0.501±0.052	23.67	0.378±0.036	36.40	0.148±0.010	47.07	93.23
	75	0.543±0.040	16.12	0.413±0.044	28.85	0.165±0.020	36.04	126.80
	37.5	0.585±0.049	8.45	0.477±0.045	15.17	0.195±0.046	15.77	132.91
4b-3	300	0.385±0.044	44.69	0.286±0.046	55.98	0.133±0.023	57.66	79.92
	150	0.436±0.035	35.57	0.340±0.047	44.44	0.149±0.033	46.40	92.59
	75	0.487±0.042	26.27	0.404±0.050	30.63	0.172±0.033	30.86	93.38
	37.5	0.537±0.047	17.15	0.445±0.036	21.94	0.181±0.031	24.77	100.48
4c-1	300	0.213±0.021	75.85	0.133±0.023	88.68	0.080±0.009	93.02	35.15
	150	0.280±0.017	63.83	0.171±0.018	80.48	0.089±0.007	86.94	53.83
	75	0.312±0.046	57.97	0.233±0.039	67.31	0.102±0.024	78.38	72.91
	37.5	0.431±0.012	36.41	0.289±0.036	55.41	0.113±0.023	70.72	79.27
4c-2	300	0.313±0.053	57.85	0.176±0.018	79.49	0.092±0.014	85.36	43.05
	150	0.395±0.043	42.93	0.219±0.022	70.37	0.114±0.020	70.50	73.81
	75	0.460±0.026	31.22	0.292±0.028	54.63	0.130±0.025	59.46	85.51
	37.5	0.509±0.029	22.34	0.401±0.046	31.48	0.170±0.028	32.43	94.40
4c-3	300	0.310±0.012	58.27	0.138±0.026	87.54	0.088±0.007	88.06	79.40

	150	0.377±0.043	46.26	0.252±0.025	63.25	0.125±0.023	63.06	92.17
	75	0.455±0.037	32.13	0.336±0.029	45.37	0.141±0.006	52.03	104.98
	37.5	0.520±0.035	20.35	0.410±0.036	29.56	0.174±0.031	29.73	112.39
4d-1	300	0.309±0.022	58.51	0.190±0.029	76.57	0.098±0.015	81.31	67.22
	150	0.404±0.041	41.25	0.269±0.031	59.62	0.114±0.018	70.05	82.84
	75	0.482±0.038	27.17	0.343±0.046	43.87	0.121±0.016	65.77	94.16
	37.5	0.537±0.028	17.21	0.430±0.038	25.28	0.173±0.030	30.41	101.03
4d-2	300	0.267±0.041	66.18	0.217±0.031	70.66	0.104±0.014	77.18	89.29
	150	0.321±0.038	56.28	0.274±0.031	58.55	0.118±0.016	67.34	91.49
	75	0.418±0.036	38.77	0.360±0.044	40.10	0.133±0.022	57.66	95.37
	37.5	0.509±0.048	22.28	0.431±0.029	24.93	0.164±0.023	36.49	109.10
4d-3	300	0.305±0.020	59.30	0.233±0.020	67.31	0.103±0.004	77.93	95.61
	150	0.375±0.044	46.62	0.311±0.035	50.71	0.117±0.016	68.24	97.46
	75	0.436±0.040	35.45	0.373±0.019	37.39	0.135±0.028	56.08	107.07
	37.5	0.527±0.039	19.08	0.439±0.051	23.29	0.174±0.039	29.73	119.12

221

222

223 Table 2. Effects of on the inhibition of HBeAg secretion by HepG2.2.15 cells ($\bar{x}$±s, n=3).

Groups	Concentration/ μM	3 days		6 days		9 days		9 days
		OD ($\bar{x}$±s)	Inhibition (%)	OD ($\bar{x}$±s)	Inhibition (%)	OD ($\bar{x}$±s)	Inhibition (%)	Cell survival (%)
Control	-	3.502±0.030	-	3.455±0.018	-	2.619±0.050	-	100
3TC	300	2.441±0.218	30.87	2.100±0.186	39.92	1.079±0.063	60.17	75.19
	150	2.680±0.310	23.93	2.398±0.216	31.12	1.458±0.089	45.36	82.39
	75	2.983±0.353	15.09	2.706±0.297	22.05	1.745±0.147	34.17	95.86
	37.5	3.154±0.320	10.13	3.021±0.224	12.78	2.148±0.242	18.39	118.45
4a-1	300	1.771±0.212	50.35	1.522±0.091	56.93	1.104±0.156	59.20	99.54
	150	2.241±0.211	36.68	1.846±0.250	47.38	1.381±0.141	48.38	101.86
	75	2.550±0.272	27.71	2.339±0.180	32.88	1.589±0.099	40.34	104.25
	37.5	2.837±0.258	19.34	2.617±0.101	24.69	1.927±0.127	27.04	106.67
4a-2	300	2.065±0.373	41.81	1.799±0.263	48.79	0.171±0.174	56.60	103.31
	150	2.457±0.359	30.39	2.030±0.175	41.97	1.500±0.159	43.74	114.02
	75	2.875±0.292	18.25	2.507±0.153	27.91	1.665±0.211	37.28	120.16
	37.5	3.019±0.221	14.06	2.776±0.321	20.01	1.927±0.087	27.03	128.25
4a-3	300	3.009±0.213	14.35	2.252±0.315	35.44	1.281±0.397	52.27	97.71
	150	3.098±0.359	11.75	2.763±0.242	20.37	1.912±0.223	26.95	98.65
	75	3.260±0.335	7.04	2.936±0.296	15.29	2.042±0.194	22.55	101.20
	37.5	2.480±0.029	0.63	3.164±0.175	8.58	2.142±0.188	18.65	113.67
4b-1	300	2.325±0.158	34.24	1.634±0.226	53.64	1.055±0.047	61.10	88.95
	150	2.532±0.257	28.22	2.264±0.205	35.09	1.394±0.217	47.87	98.07
	75	2.804±0.238	20.31	2.462±0.249	29.24	1.565±0.095	41.17	106.92

	37.5	3.042±0.308	13.38	2.730±0.264	21.35	1.847±0.207	30.16	108.25
4b-2	300	2.498±0.213	29.21	2.009±0.121	42.59	1.135±0.085	58.00	76.08
	150	2.726±0.279	22.58	2.291±0.222	34.28	1.464±0.136	45.12	93.23
	75	3.048±0.210	13.21	2.580±0.240	25.76	1.707±0.119	35.64	126.80
	37.5	3.310±0.133	5.59	2.847±0.243	17.91	1.970±0.155	25.35	132.91
4b-3	300	2.975±0.272	15.34	2.331±0.292	33.10	1.210±0.153	55.06	79.92
	150	3.113±0.246	11.32	2.497±0.174	28.22	1.435±0.142	46.26	92.59
	75	3.205±0.289	8.64	2.744±0.231	20.93	1.811±0.164	31.56	93.38
	37.5	3.521±0.033	-	2.876±0.221	17.06	2.091±0.161	20.62	100.48
4c-1	300	1.321±0.167	63.46	0.567±0.028	85.08	0.152±0.047	96.42	35.15
	150	1.582±0.137	55.85	0.819±0.054	77.64	0.164±0.034	95.92	53.83
	75	1.870±0.130	47.47	0.914±0.021	74.84	0.321±0.055	89.79	72.91
	37.5	2.412±0.030	31.70	1.198±0.132	66.47	0.508±0.051	82.51	79.27
4c-2	300	1.878±0.242	47.24	1.043±0.239	71.05	0.400±0.041	86.70	43.05
	150	2.293±0.085	35.18	1.538±0.150	56.47	1.108±0.128	59.06	73.81
	75	2.651±0.382	24.76	1.900±0.272	45.80	1.417±0.185	46.96	85.51
	37.5	2.922±0.288	16.88	2.574±0.244	25.96	1.844±0.157	30.27	94.40
4c-3	300	1.740±0.207	51.27	1.308±0.182	63.25	0.787±0.083	71.60	79.40
	150	2.352±0.214	33.45	1.890±0.246	46.09	1.302±0.154	51.48	92.17
	75	2.620±0.249	25.67	2.368±0.199	32.02	1.522±0.167	42.86	104.98
	37.5	2.957±0.150	15.86	2.757±0.213	20.55	1.969±0.122	25.41	112.39
4d-1	300	1.640±0.158	54.17	0.895±0.014	75.41	0.506±0.023	82.58	67.22
	150	1.939±0.288	45.48	1.298±0.090	63.53	0.949±0.080	65.26	82.84
	75	2.565±0.251	27.27	2.018±0.251	42.34	1.153±0.105	57.29	94.16
	37.5	2.891±0.171	17.77	2.686±0.311	22.66	1.852±0.261	29.99	101.03
4d-2	300	1.448±0.194	59.76	1.352±0.165	61.95	0.711±0.097	74.57	89.29
	150	1.730±0.204	51.55	1.571±0.134	55.48	0.952±0.098	65.16	91.49
	75	2.400±0.185	32.07	2.171±0.231	37.82	1.162±0.088	56.92	95.37
	37.5	2.646±0.267	24.92	2.413±0.225	30.69	1.825±0.089	31.04	109.10
4d-3	300	2.062±0.209	41.91	1.719±0.087	51.13	0.936±0.199	65.75	95.61
	150	2.341±0.124	33.77	2.097±0.228	40.00	1.138±0.041	57.87	97.46
	75	2.624±0.338	25.55	2.309±0.104	33.75	1.367±0.156	48.93	107.07
	37.5	3.064±0.358	12.73	2.908±0.267	16.10	1.871±0.172	29.22	119.12

224
225
226
227
228
229
230
231
232
233
234

235 Table 3. Effects of on the inhibition of HBV DNA replication ($\bar{x}\pm s\times10^2$, n=3).

Groups	Concentration/ μM	3 days		6 days		9 days	
		HBV DNA (copies/μl)	Inhibition (%)	HBV DNA (copies/μl)	Inhibition (%)	HBV DNA (copies/μl)	Inhibition (%)
Control	-	9.19±1.22	-	10.50±0.78	-	10.91±0.92	-
3TC	300	3.73±0.19	59.45	2.89±0.63	71.59	1.48±0.51	86.39
	150	4.91±0.27	46.61	3.48±0.61	66.83	2.00±0.98	81.64
	75	4.97±0.21	45.96	4.32±0.71	58.89	2.54±0.95	76.68
	37.5	5.52±0.28	39.97	6.45±0.93	38.57	3.34±0.49	69.42
4c-1	300	3.42±0.37	62.82	3.28±0.12	68.79	1.55±0.54	85.82
	150	4.98±0.33	45.77	4.03±0.95	61.59	3.03±0.52	72.22
	75	5.80±0.35	36.89	5.50±0.78	47.62	3.41±0.55	68.73
	37.5	6.40±0.26	30.36	6.50±0.53	38.10	4.53±0.50	58.44
4d-1	300	5.42±0.37	41.06	4.94±0.46	52.92	3.55±0.47	67.48
	150	5.98±0.33	34.89	5.80±0.44	44.76	4.96±0.49	54.49
	75	6.57±0.65	28.55	6.38±0.28	39.21	5.74±0.14	47.34
	37.5	7.20±0.50	21.65	7.67±0.13	26.95	6.90±0.52	36.74
4d-2	300	4.92±0.44	46.50	4.48±0.55	57.37	4.20±0.26	61.49
	150	5.45±0.13	40.70	6.00±0.46	42.86	5.23±0.42	52.02
	75	6.48±0.26	29.45	6.37±0.38	39.37	6.58±0.29	39.64
	37.5	7.37±0.42	19.84	7.60±0.10	27.62	7.58±0.19	30.47

236